Electronic Journal of Differential Equations, Vol. 2012 (2012), No. 160, pp. 1–30.
ISSN: 1072-6691. URL: http://ejde.math.txstate.edu or http://ejde.math.unt.edu
ftp ejde.math.txstate.edu

PATTERN FORMATION IN A MIXED LOCAL AND NONLOCAL REACTION-DIFFUSION SYSTEM

EVELYN SANDER, RICHARD TATUM

Abstract. Local and nonlocal reaction-diffusion models have been shown to demonstrate nontrivial steady state patterns known as Turing patterns. That is, solutions which are initially nearly homogeneous form non-homogeneous patterns. This paper examines the pattern selection mechanism in systems which contain nonlocal terms. In particular, we analyze a mixed reaction-diffusion system with Turing instabilities on rectangular domains with periodic boundary conditions. This mixed system contains a homotopy parameter β to vary the effect of both local ($\beta = 1$) and nonlocal ($\beta = 0$) diffusion. The diffusion interaction length relative to the size of the domain is given by a parameter ϵ. We associate the nonlocal diffusion with a convolution kernel, such that the kernel is of order $\epsilon^{-\theta}$ in the limit as $\epsilon \to 0$. We prove that as long as $0 \leq \theta < 1$, in the singular limit as $\epsilon \to 0$, the selection of patterns is determined by the linearized equation. In contrast, if $\theta = 1$ and β is small, our numerics show that pattern selection is a fundamentally nonlinear process.

1. Introduction

Turing in 1952 first suggested a mechanism in which chemicals, through the process of diffusion, could form highly developed patterns [35]. Now referred to as Turing patterns, they have been experimentally shown in several well-known reaction-diffusion systems such as the chlorite-iodide-malonic acid (CIMA) reaction [24], and more recently, the Belousov-Zhabotinsky (BZ) reaction using a water-in-oil aerosol micro-emulsion [36]. Prior to this important discovery, Field and Noyes devised the well-known Oregonator reaction-diffusion equation for the Belousov-Zhabotinsky (BZ) reaction [13]. However, these models do not account for any nonlocal interactions. Using a nonlocal feedback illuminating source, Hildebrand, Skødt and Showalter [19] experimentally showed the existence of novel spatiotemporal patterns in the BZ reaction. This system is similar to System (1.1) the equation we consider in this paper, except that the version we consider does not contain a thresholding function. In particular, we consider the following system of equations

2000 *Mathematics Subject Classification.* 35B36, 35K57.
Key words and phrases. Reaction-diffusion system; nonlocal equations; Turing instability; pattern formation.

Submitted March 19, 2012. Published September 20, 2012.

subject to periodic boundary conditions:

$$\begin{aligned} u_t &= \epsilon(\beta\Delta u + (1-\beta)(J*u - \hat{J}_0\cdot u)) + f(u,v),\\ v_t &= d\epsilon(\beta\Delta v + (1-\beta)(J*v - \hat{J}_0\cdot v)) + g(u,v) \end{aligned}, \tag{1.1}$$

where $\Omega \subset \mathbb{R}^n$ is a rectangular domain for $n \in \{1,2,3\}$ and u and v model concentrations of activator and inhibitor populations, respectively. This equation contains a homotopy between pure local diffusion and a nonlocal counterpart with the homotopy parameter $\beta \in [0,1]$. The convolution is defined by

$$J*u(x,t) = \int_\Omega J(x-y)u(y,t)dy, \tag{1.2}$$

$$\hat{J}_0 = \frac{1}{|\Omega|}\int_\Omega J(x)dx, \tag{1.3}$$

where the kernel $J : \mathbb{R}^n \to \mathbb{R}$ of the convolution is periodic. The kernel J is assumed to be such that for some $0 \le \theta \le 1$, $\epsilon^\theta J(x)$ limits uniformly to a smooth ϵ-independent function $K(x)$ as $\epsilon \to 0$. For our simulations, we use a Gaussian kernel that is modified by a smooth cut-off function similar to the kernel used in [17]. See Appendix A for more details about the kernel choice. In System (1.1), diffusion is modeled by the local and nonlocal operators, while the nonlinearities model the associated reaction kinetics. System (1.1) includes both local and nonlocal operators to model both short and long range diffusion effects [28]. The inclusion of both operators in the model is important for those physical systems in which both effects are present. Again, see [19]. The parameter d is the ratio of the diffusion coefficients of u and v, in which higher values of d indicate higher diffusion rates for the inhibitor species. The parameter ϵ is a scale parameter that regulates the effects of the reaction kinetics over the domain Ω.

For a large range of nonlinear functions f and g, the system above has an unstable spatially homogeneous equilibrium $(\bar{u}_0, \bar{v}_0)$ (See Lemma 2.13). This corresponds to an experimental or naturally occurring setting in which the uniformly mixed starting state is destabilized by small fluctuations. In order to study how these natural fluctuations impact the evolving mixture, one studies the time evolution of solutions starting at initial conditions close to the homogeneous equilibrium. After a rather short time, such solutions form patterns. However, even for a fixed set of parameters, every initial condition results in different pattern formation. Thus through the initial condition, randomness enters an otherwise deterministic process of pattern formation. Although the fine structure of these patterns differ, the patterns exhibit common characteristic features and similar wavelength scales. In this paper, we concentrate on understanding the key features of these patterns under nonlocal diffusion.

This paper focuses on short term pattern formation rather than asymptotic behavior. See Figure 1. In most natural systems, not only the asymptotic behavior but also the transient patterns that occur dynamically are critically important for understanding the behavior of the system. For example, in cases of metastability [2], the convergence to the global minimizers is exponentially long, and thus from a practical point of view not viable. More generally, many systems simply never reach equilibrium on the time scale of the natural problems. To quote Neubert, Caswell, and Murray [30]: "Transient dynamics have traditionally received less attention than the asymptotic properties of dynamical systems. This reflects the

difficulty in studying transients, the belief that dynamics are more important than history, and the mistaken belief that asymptotic properties completely characterize the solution. ... There is, however, a growing recognition that transient dynamics deserve more study."

We specifically consider the pattern formation occurring in the limit as ϵ approaches zero. The parameter ϵ is a measure of the interaction length of diffusion on a fixed domain. A rescaling of the time $\tilde{t} = \epsilon t$ and setting $\gamma = 1/\epsilon$, where we drop the tilde after rescaling, results in the system of equations: $u_t = (\beta\Delta u + (1-\beta)(J*u - \hat{J}_0 \cdot u)) + \gamma f(u,v)$, $v_t = d(\beta\Delta v + (1-\beta)(J*v - \hat{J}_0 \cdot v)) + \gamma g(u,v)$. In this form, γ is viewed as a measure of the domain size. See for example Murray [28].

A standard heuristic explanation of the pattern formation starting near the homogeneous equilibrium is to say that the patterns can be fully explained by considering only the eigenfunction corresponding to the most unstable eigenvalue of the linearization (which we will refer to as the most unstable eigenfunction). For example, such an explanation was given by Murray [28] for the above equation in the case that $\beta = 1$. The same explanation was given for spinodal decomposition for the Cahn-Hilliard equation by Grant [15]. However, this explanation does not explain the patterns that are seen: most unstable eigenfunctions are regularly spaced periodic patterns, whereas the patterns seen are irregular snake-like patterns with a characteristic wavelength. This discrepancy arises because the most unstable eigenfunction only describes pattern formation for solutions that start exponentially close to the homogeneous equilibrium, whereas both numerical and experimental pattern formation can at best be considered as polynomially close to the equilibrium. Sander and Wanner [33] gave an explanation for the irregular patterns for solutions for the above equation in the case of purely local diffusion (i.e. for $\beta = 1$), and in this paper, we have extended these results to the case of nonlocal diffusion. See Fig. 2. By applying [25, 26], Sander and Wanner showed that the observed patterns arise as random superpositions of a finite set of the most unstable eigenfunctions on the domain called the *dominating subspace*. These results are not merely a use of simple linearization techniques, which would give only topological rather than quantitative information as to the degree of agreement between linear and nonlinear solutions. Using "most nonlinear patterns" approach of Maier-Paape and Wanner [25], it is possible to show both the dimension of the dominating subspace, and the degree to which linear and nonlinear solutions agree. In particular, the technique shows there exists a finite-dimensional inertial manifold of the local reaction-diffusion system which exponentially attracts all nearby orbits. The orbit can be projected onto this finite-dimensional manifold. In this paper, we extend their results to the mixed local-nonlocal equation given in (1.1). Our results are the first generalization of the results obtained in [33] to nonlocal reaction-diffusion systems.

We now state our main theoretical result. In order to compare solutions to the nonlinear equation (1.1) and of the linearization of this equation linearized at the homogeneous equilibrium $(\bar{u}_0, \bar{v}_0)$, let (u,v) denote a solution to the full nonlinear equation starting at initial condition (u_0, v_0), and let $(u_{\text{lin}}, v_{\text{lin}})$ denote a solution to the linearized equation starting at the same initial condition. We consider initial conditions which are a specified distance r_ϵ from the homogeneous equilibrium depending only on ϵ. We refer to this value r_ϵ as the *initial radius*. The subscript

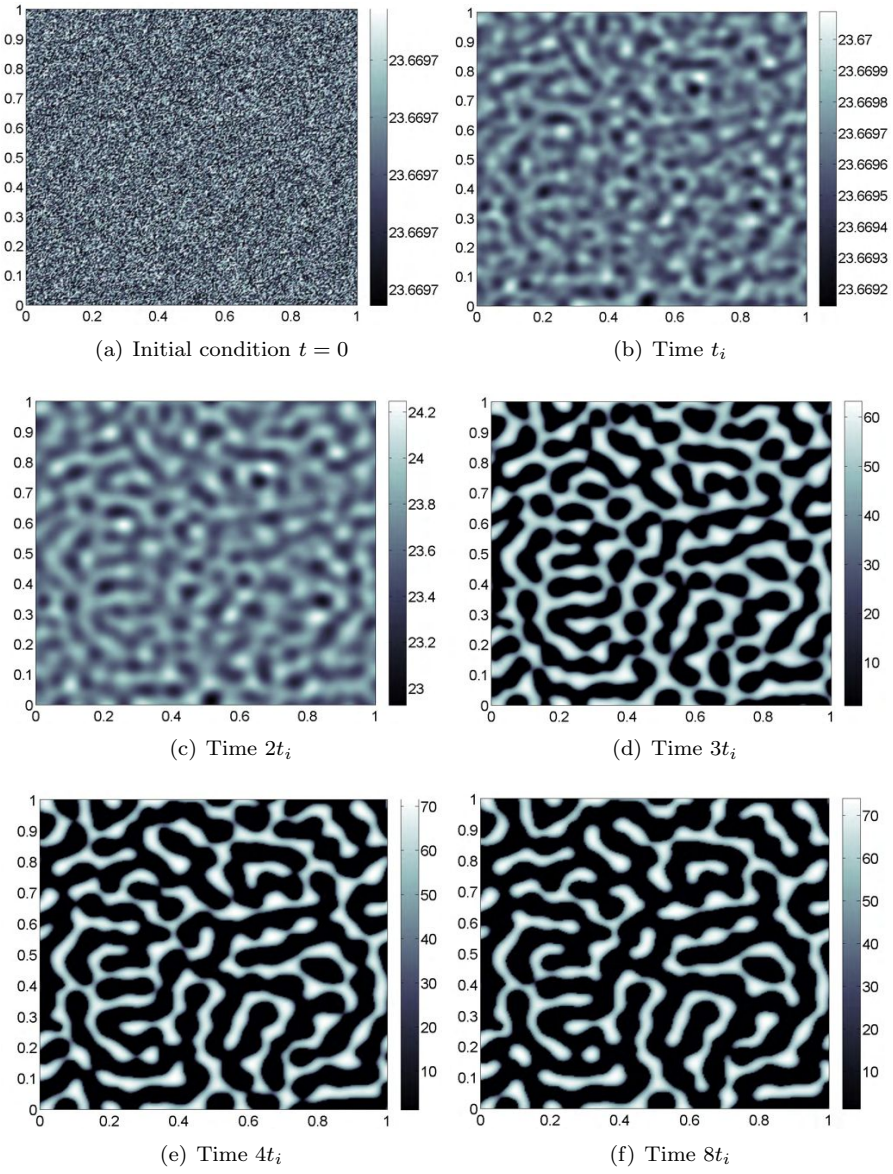

FIGURE 1. Early and later pattern formation with $\beta = 0$. Starting with an initial random perturbation about the homogeneous equilibrium (a), the system evolves to show pattern formation after $t_i = 2.23 \times 10^{-3}$ time units. The behavior seen in (b)-(c) is the focus of our results. Further pattern formation development occurs in (d)-(e).

denotes the fact that the choice of initial radius varies with ϵ. We compare the trajectories of (u, v) and $(u_{\text{lin}}, v_{\text{lin}})$ until the distance between the solution (u, v) and the homogeneous equilibrium (u_0, v_0) reaches the *exit radius* value R_ϵ. Clearly

we choose $R_\epsilon > r_\epsilon$. When the solution has reached the exit radius, we measure the *relative distance*

$$D_\epsilon := \frac{\|(u(t), v(t)) - (\bar{u}_0, \bar{v}_0) - (u_{\text{lin}}, v_{\text{lin}})\|_{**}}{\|(u_{\text{lin}}(t), v_{\text{lin}}(t))\|_{**}}.$$

The $\|\cdot\|_{**}$-norm is equivalent to the standard Sobolev norm. See Lemma 4.5 of Section 4. If it is possible to choose the initial radius such that $r_\epsilon \to 0$ as $\epsilon \to 0$ and the exit radius such that $R_\epsilon \to \infty$ as $\epsilon \to 0$, such that $D_\epsilon \to 0$ as $\epsilon \to 0$, this implies that as ϵ limits to zero, the nonlinear behavior of solutions is progressively closer to linear as $\epsilon \to 0$. We refer to this as *almost linear behavior*.

Extending techniques in [25, 26, 33], we give conditions such that the mixed system given by System (1.1) displays almost linear behavior. Our main theoretical result is summarized in the following theorem.

Theorem 1.1. *Let $\epsilon < \epsilon_0$ and choose α such that $\dim\Omega/4 < \alpha < 1$. Assume that System (1.1) satisfies the following conditions:*

(1) *Ω is a rectangular domain of $\mathbb{R}^n$, where $n = \{1, 2, 3\}$.*
(2) *The nonlinearities f and g are sufficiently smooth and satisfy Turing instability conditions with real eigenvalues. Namely, they satisfy conditions such that the eigenvalues of the linearized right hand side of System (1.1) are real; in addition, f are g are assumed to be such that for $\epsilon = 0$, the system is stable, and there exists an $\epsilon_0 > 0$ such that for all $0 < \epsilon \le \epsilon_0$, the homogeneous equilibrium $(\bar{u}_0, \bar{v}_0)$ is unstable. (These conditions are given in Lemma 2.13 and Assumption 2.14).*
(3) *For some constant $0 \le \theta \le 1$, the limit of the kernel function*

$$K(x) = \lim_{\epsilon \to 0} \epsilon^\theta J(x)$$

is a uniform limit to a C^1 smooth $\epsilon-$independent function, which is smoothly periodic with respect Ω.
(4) *Define $\hat{K}_0 = \int_\Omega K(x)\,dx$. For β satisfying $0 < \beta < 1$ and two constants $s_\ell < s_r$ determined by the functions f and g (defined in 3.14), we assume that $\hat{K}_0$ satisfies the condition*

$$s_r < \hat{K}_0 < \frac{s_\ell}{\epsilon^{1-\theta} \cdot (1-\beta)}.$$

as $\epsilon \to 0$.

We define the constant χ to be a measure of the order of the nonlinearity of the functions f and g (defined in 4.12). Then there is almost linear behavior with the following values of the constants $r_\epsilon, R_\epsilon, D_\epsilon$ defined above:

$$0 < r_\epsilon \sim \min(1, (\epsilon^{-(\alpha - \dim\Omega/4) + \alpha/\chi + \xi})^{1/(1-\xi)}),$$
$$0 < R_\epsilon \sim \epsilon^{-(\alpha - \dim\Omega/4) + \alpha/\chi + \xi},$$
$$D_\epsilon \sim \epsilon^{\alpha - \dim\Omega/4}.$$

The results of the above theorem are schematically depicted in Figure 3. The value θ describes the asymptotic ϵ-dependent relationship between $J(x)$ and an ϵ-independent kernel $K(x)$. Hypothesis 4 of the theorem states that for fixed $\hat{K}_0$, f, and g, if $0 \le \theta < 1$ then any β value between 0 and 1 is sufficient for the results of the theorem to hold. However, if $\theta = 1$, then β must be sufficiently close to 1 for the results to follow. This can be clearly seen numerically in Figures 4-6.

The parameters of the nonlinearity featured in Figure 4 can be found in [33] and are known to give rise to Turing instability under the appropriate choice for ϵ and d. See [29]. Figures 5-6 use random perturbations of the nonlocal parameters in Figure 4 that also give rise to Turing instability. Since the results are asymptotic in ϵ, the values of r, R, and D are independent of θ. As $\epsilon \to 0$, the size of θ determines how quickly the solutions display almost linear behavior.

This theorem does not mention the case in which $\theta > 1$. In this case the homogeneous equilibrium is asymptotically stable independent of any other parameter values. Therefore all random fluctuations sufficiently close to the homogeneous equilibrium converge to the homogeneous equilibrium, and there is no pattern formation. We performed numerics to see what size of fluctuations are possible in this case. Our numerics show that for fluctuations of .1, the solutions converge to the homogeneous equilibrium. The details and proof of this theorem are given in Section 4 as a combination of Theorems 4.8 and 4.10. The case of $\beta = 1$ in the above theorem is analogous to the homogeneous Neumann case considered in [33]. For $\beta < 1$, our results are new.

The numerical results in Figure 4-6 as well as our other numerical investigations (not shown here) indicate that the estimates for $\theta \to 1$ of the above theorem remain true as long as β remains in an interval $[\beta_0, 1]$, where $\beta_0 > 0$. Indeed, in the numerics the nonlinear behavior of solutions becomes more and more pronounced for small ϵ as $\theta \to 1$ outside of $[\beta, 1]$. Our numerics indicate an additional conclusion for small β (cf. Figures 4-6). Specifically, they indicate that the results of the above theorem cannot be generalized to include the case of purely nonlocal systems. For systems close to purely nonlocal (ie. $\beta < \beta_0$), the behavior becomes fundamentally nonlinear. The thesis of Hartley [16] included numerical observations of a similar distinction between local and nonlocal behavior for a phase field model with a homotopy between purely local and nonlocal terms.

Note that in the above theorem and numerics, we have used the $**$-norm to study distances since it is the natural mathematical choice. The natural physical choice is the L^∞-norm, by which measure our results are only polynomial in ϵ rather than order one. See Sander and Wanner [33] for a more detailed discussion of theoretical and numerical measurements in the two norms.

Mixed local and nonlocal equations have been considered previously. The Fisher-KPP was shown to generate traveling waves [7]. A similar model also appears in the survey article of Fife [14] and in Lederman and Wolanski [23] in the context of the propagation of flames. Hartley and Wanner also studied pattern formation for a mixed phase field model with a homotopy parameter like Eqn. (1.1) [17]. Specifically, for the stochastic nonlocal phase-field model, they used functional-analytic structure to prove the existence and uniqueness of mild solutions [17]. We use a related method here to describe the early pattern selection for Eqn. (1.1).

This paper is organized as follows. Section 2 contains our assumptions. Section 3 describes the properties of the linearization of the right hand side. The full spectrum of the linearization is given in Section 3.1. The almost linear results for System (1.1) are found in Section 4. The final section includes a summary with some conjectures.

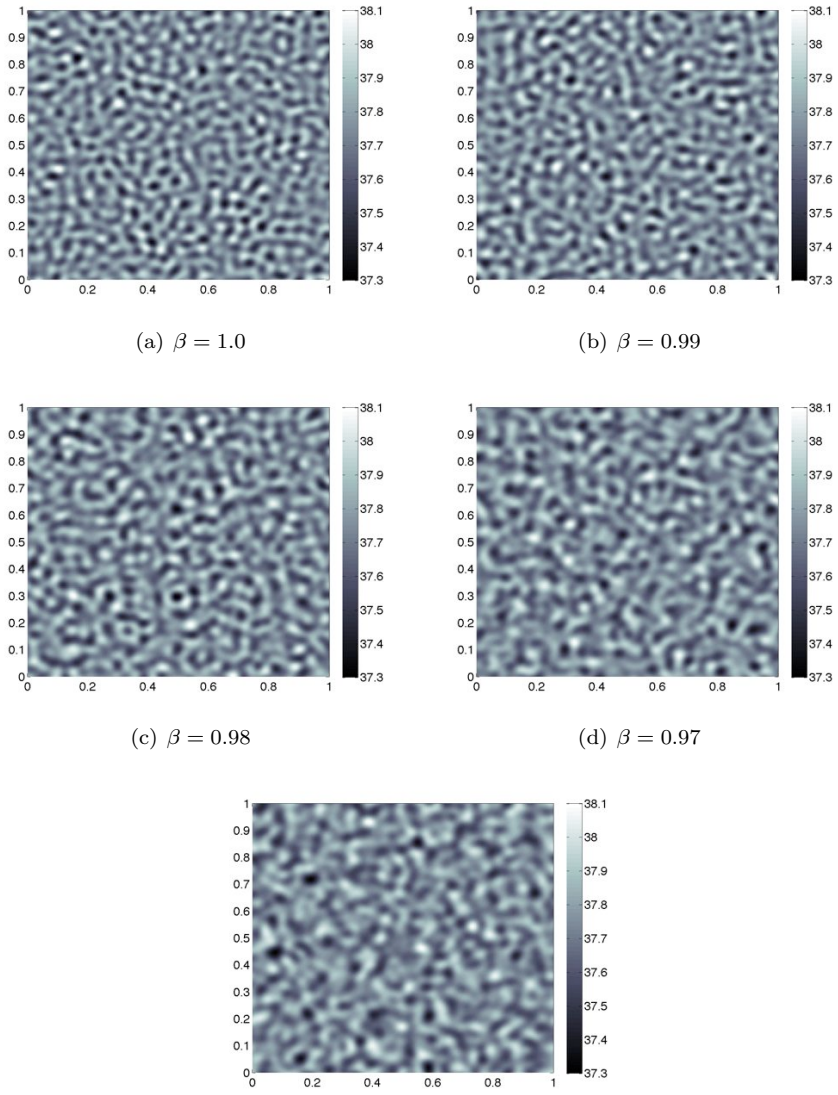

(a) $\beta = 1.0$

(b) $\beta = 0.99$

(c) $\beta = 0.98$

(d) $\beta = 0.97$

(e) $\beta = 0.96$

FIGURE 2. Examples of the patterns produced using various β values and $\epsilon = 1 \times 10^{-5}$ over the domain $[0,1]^2$. These patterns occur when the relative distance between the nonlinear and linear solution reaches a threshold value D_ϵ of 0.01. As β decreases, the characteristic size of the patterns becomes larger. Note that $(s_\ell, s_r) \approx (.0071, .8806)$. See Appendix 6 for a description of the kernel.

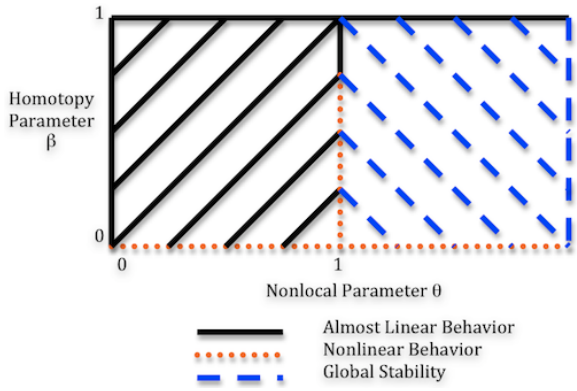

FIGURE 3. A summary of behavior in each parameter region given by Theorem 1.1.

2. Preliminaries

In this section, we describe in detail our assumptions for the domain, kernel type, smoothness of the nonlinearity, and type of instability exhibited by the homogeneous equilibrium.

Assumption 2.1 (Rectangular domain)**.** Let Ω be a closed rectangular subset of $\mathbb{R}^n$ for $n \in \{1, 2, 3\}$.

Definition 2.2 (Spectrum of $-\Delta$)**.** Suppose that Ω satisfies Assumption 2.1. Let $L^2_{\text{per}}(\Omega)$ be the space of functions which are periodic with respect to Ω and belong to $L^2(\Omega)$. For $\Delta : L^2_{\text{per}}(\Omega) \to L^2_{\text{per}}(\Omega)$, denote the ordered sequence of eigenvalues of $-\Delta$ as $0 = \kappa_0 < \kappa_1 \leq \cdots \to \infty$ [3, Section 1.3.1]. Denote the corresponding real-valued L^2-orthonormalized eigenfunctions by ψ_k, for $k \in \mathbb{N}$.

Assume that $K \in L^2_{\text{per}}(\Omega)$. An important aspect of Definition 2.2 is that we can define the Fourier series for functions J and K as

$$J_N(x) = \sum_{k=0}^{N} \hat{J}_k \psi_k(x), \quad \text{and} \quad K_N(x) = \sum_{k=0}^{N} \hat{K}_k \psi_k(x), \tag{2.1}$$

where

$$\hat{J}_k = \int_\Omega J(x)\psi_k(x)dx, \quad \text{and} \quad \hat{K}_k = \int_\Omega K(x)\psi_k(x)dx. \tag{2.2}$$

Note that if $J, K \in C^1(\bar{\Omega})$, then $J_N \to J$ and $K_N \to K$ uniformly as $N \to \infty$. See [22]. Observe that $\hat{J}_0 = \int_\Omega J(x)dx/|\Omega|$ since $\psi_0 = 1/|\Omega|$ by Definition 2.2.

Definition 2.3 (Smooth periodicity on Ω)**.** Suppose that Ω satisfies Assumption 2.1. A function $f : \Omega \to \mathbb{R}$ is said to be smoothly periodic on Ω if it is periodic with respect to the boundary $\partial\Omega$ and can be extended to a smooth function on $\mathbb{R}^n$.

Assumption 2.4 (The kernel function J and its limit K)**.** Suppose that Ω satisfies Assumption 2.1. Let the kernel $J \in C^1(\bar{\Omega})$ be such that for some $0 \leq \theta \leq 1$, there is an ϵ-independent function $K(x)$ such that $K(x) = \lim_{\epsilon \to 0} \epsilon^\theta \cdot J(x)$, where the limit is a uniform limit. Assume that $J(x)$ and $K(x)$ are smoothly periodic on Ω.

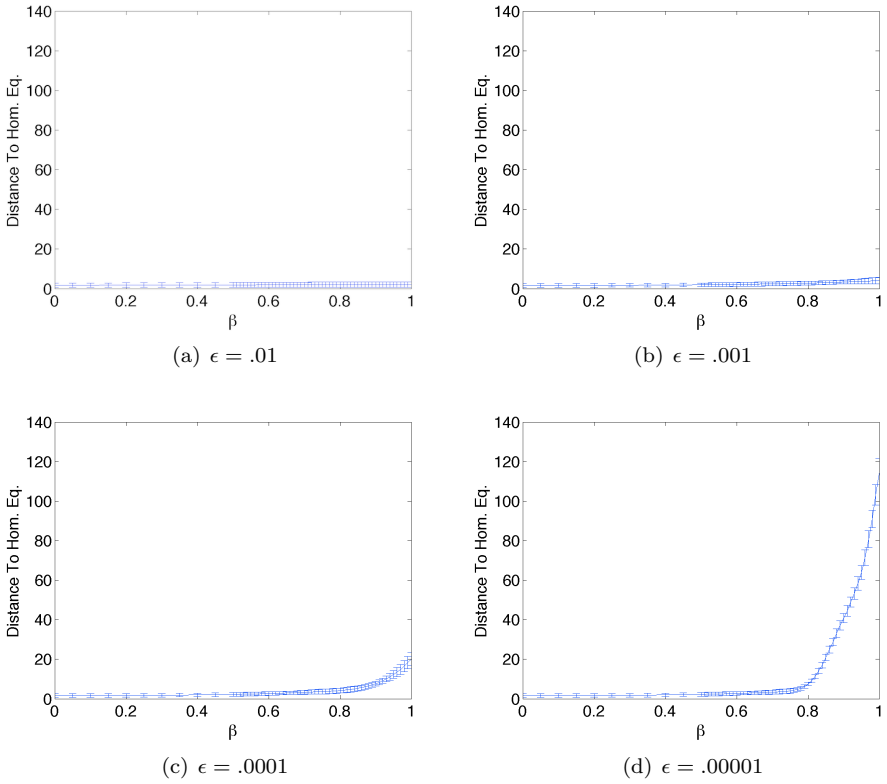

(a) $\epsilon = .01$ (b) $\epsilon = .001$

(c) $\epsilon = .0001$ (d) $\epsilon = .00001$

FIGURE 4. Exit radius R_ϵ for relative distance 0.01, varied β and nonlinearity parameters $a = 150.0$, $b = 100.0$, $\rho = 13.0$, $A = 1.5$, and $K = 0.050$. For each simulation, we used random initial conditions with initial radius $r_\epsilon < \epsilon^{1/4}$. As $\beta \to 0$, the measured values are smaller, meaning that the behavior of solutions is determined by nonlinear effects. This is more pronounced for smaller ϵ values. For each β and ϵ value depicted we performed 20 distinct simulations. Distances are measured in the $\|\cdot\|_{**}$ norm, as defined in Section 4. To capture the rapid change in the graph, a refined grid is used near $\beta = 1$. In all simulations, we used a Galerkin spectral method with a semi-implicit 2D integration scheme that used 128^2 nodes. Note that $(s_\ell, s_r) \approx (.0071, .8806)$. See Appendix 6 for a description of the kernel.

Furthermore, assume the Fourier coefficients are such that $\hat{K}_0 > \hat{K}_k$ for all $k > 0$, and thus $\hat{J}_0 > \hat{J}_k$ for ϵ sufficiently small.

The meaning of the convolution operator on $\mathbb{R}^n$ is well established, but convolution on Ω is not. The following definition specifies what is meant here by convolution of functions on Ω.

Definition 2.5 (Convolution on Ω)**.** Suppose that K and J satisfy Assumption 2.4 and that the periodic extension of K and J are given as K_{per} and J_{per}, respectively.

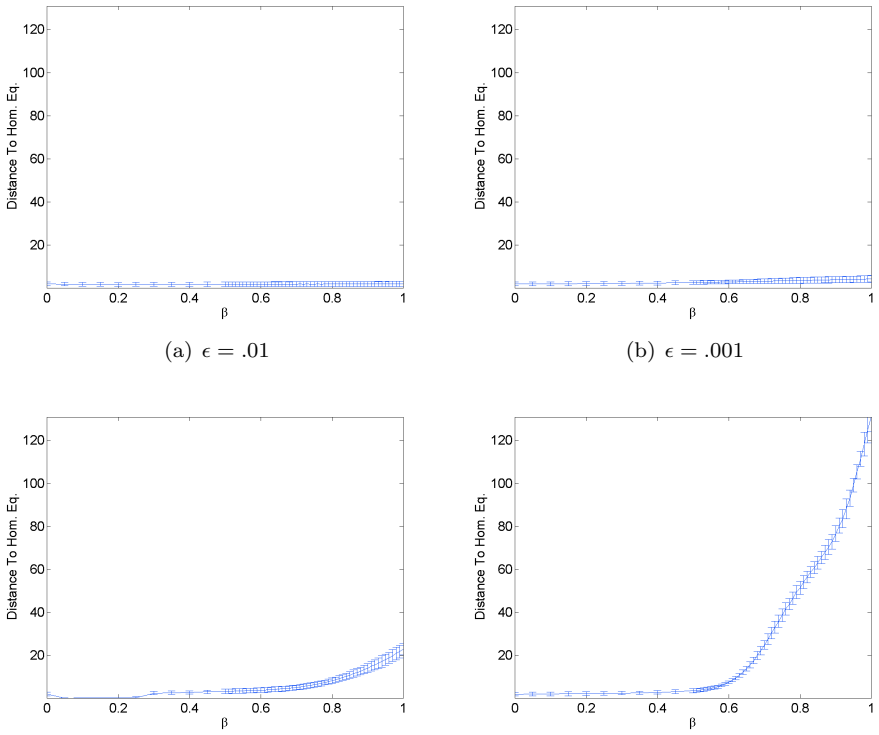

(a) $\epsilon = .01$ (b) $\epsilon = .001$

(c) $\epsilon = .0001$ (d) $\epsilon = .00001$

FIGURE 5. Exit radius R_ϵ for relative distance 0.01, varied β and nonlinearity parameters $a = 127.0$, $b = 81.0$, $\rho = 29.0$, $A = 1.5$, and $K = 0.040$. For each simulation, we used random initial conditions with initial radius $r_\epsilon < \epsilon^{1/4}$. As with the nonlinearity parameters associated with Figure 5, we see that the solutions are dominated by nonlinearity effects as $\beta \to 0$. This is more pronounced for smaller ϵ values. For each β and ϵ value depicted we performed 20 distinct simulations. Distances are measured in the $\|\cdot\|_{**}$ norm, as defined in Section 4.

The convolution of K and u is defined as

$$K_c(u) = K * u = \int_\Omega K_{\text{per}}(x-y)u(y)dy,$$

where $K_c : L^2_{\text{per}}(\Omega) \to L^2_{\text{per}}(\Omega)$ and the convolution of J and u is defined as

$$J_c(u) = J * u = \int_\Omega J_{\text{per}}(x-y)u(y)dy,$$

where $J_c : L^2_{\text{per}}(\Omega) \to L^2_{\text{per}}(\Omega)$

We now consider the adjoints of K_c and J_c. In particular, the adjoint of J_c will be used in Section 3 to describe the spectrum of the linearization of System (1.1), while the adjoint of K_c will be used in Section 4 to describe the unstable interval for

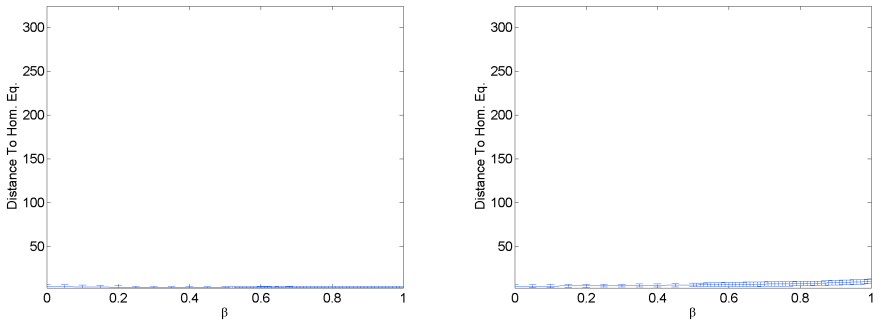

(a) $\epsilon = .01$

(b) $\epsilon = .001$

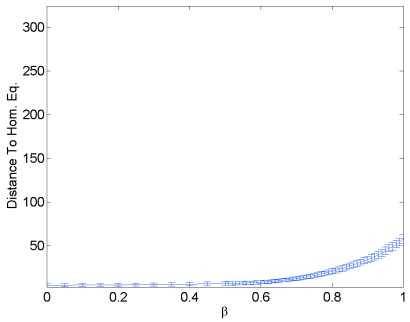

(c) $\epsilon = .0001$

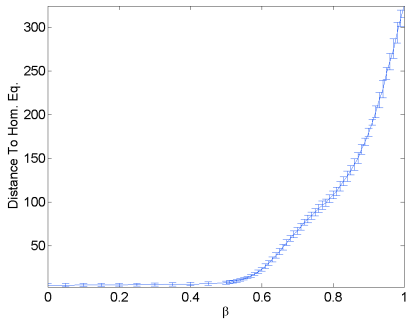

(d) $\epsilon = .00001$

FIGURE 6. Exit radius R_ϵ for relative distance 0.01, varied β and nonlinearity parameters $a = 125.5$, $b = 76.0$, $\rho = 15.2$, $A = 1.68$, and $K = 0.053$. For each simulation, we used random initial conditions with initial radius $r_\epsilon < \epsilon^{1/4}$. Qualitatively, we again see that the results do not change with changing the parameters of the nonlinearities. For each β and ϵ value depicted we performed 20 distinct simulations. Distances are measured in the $\|\cdot\|_{**}$ norm, as defined in Section 4.

which our main results hold. Let K_{per} and J_{per} be the smooth periodic extensions of K and J, respectively. We begin by defining A^K_{per} such that

$$A^K_{\text{per}}(x) = K_{\text{per}}(-x) \tag{2.3}$$

and A^J_{per} such that

$$A^J_{\text{per}}(x) = J_{\text{per}}(-x) \tag{2.4}$$

The convolution of A^K with u and A^J with u are given by

$$A^K_c(u) = A^K * u = \int_\Omega A^K_{\text{per}}(y-x)u(x)dx, \tag{2.5}$$

$$A^J_c(u) = A^J * u = \int_\Omega A^J_{\text{per}}(y-x)u(x)dx, \tag{2.6}$$

Lemma 2.6. *Suppose that Assumptions 2.1 - 2.4 are satisfied with A_c^K is defined as in* (2.5) *and A_c^J is defined as in* (2.6)*. The adjoint of K_c is A_c^K and the adjoint of J_c is A_c^J.*

Proof. As the computation of the adjoints of K_c and J_c are similar, we only show the computation of the adjoint of K_c. Let $u, v \in L^2_{\text{per}}(\Omega)$. Computing the inner product directly gives

$$\begin{aligned}(K_c(u), v) &= \int_\Omega K_c(u(x)) \cdot v(y)\, dy,\\ &= \int_\Omega \int_\Omega K_{\text{per}}(y-x) \cdot u(x) \cdot v(y)\, dx\, dy.\end{aligned}$$

Switching the order of integration, we have

$$\begin{aligned}(K_c(u), v) &= \int_\Omega \int_\Omega K_{\text{per}}(y-x) \cdot u(x) \cdot v(y)\, dy\, dx,\\ &= \int_\Omega u(x) \Big(\int_\Omega K_{\text{per}}(y-x) \cdot v(y)\, dy \Big)\, dx,\\ &= \int_\Omega u(x) \Big(\int_\Omega A^K_{\text{per}}(x-y) \cdot v(y)\, dy \Big)\, dx,\\ &= (u, A_c^K(v)).\end{aligned}$$

□

By Lemma 2.6, in order to guarantee that K_c is self-adjoint, we must use an even kernel function.

Definition 2.7. Let $T : \mathbb{R}^n \to \mathbb{R}$ and $x = (x_1, x_2, \dots, x_n) \in \mathbb{R}^n$. The function T is even if for each $x_i < 0$, $0 \le i \le n$,

$$T(x_1, x_2, \dots, x_i, \dots, x_n) = T(-x_1, -x_2, \dots, -x_i, \dots, -x_n).$$

Assumption 2.8. Suppose that J_{per} is even.

Lemma 2.9. *Suppose that Assumptions 2.1 - 2.8 are satisfied, and A_c^K and A_c^J are defined as in* (2.5) *and* (2.6)*, respectively. Then K_c and J_c are self-adjoint operators.*

Proof. By Lemma 2.6, A_c^K is the adjoint operator of K_c. Since J is such that J_{per} satisfies Assumption 2.8 and K is defined as the limit function of $\epsilon^\theta \cdot J$ in Assumption 2.4, $K_{\text{per}}(x) = K_{\text{per}}(-x)$. Thus $A_c^K = K_c$ and K_c is self-adjoint. Since J_{per} is also even by Assumption 2.8, the same reasoning shows that J_c is also self-adjoint. □

As pointed out in [17], the convolution of K with u has the same eigenfunctions as $-\Delta$.

Lemma 2.10 (Spectrum of J_c and K_c)**.** *Suppose that Ω satisfies Assumption 2.1, and that K satisfies Assumptions 2.4 - 2.8. Then the following statements are true:*

(1) $\hat{K}_k \to 0$ *as* $k \to \infty$.
(2) *The spectrum of K_c contains only the $\hat{K}_k$ and* 0*, where* 0 *is a limit point of the $\hat{K}_k$.*
(3) *For each fixed ϵ, the above statements hold for J_c as well.*

Proof. For part 1, $K \in C^1(\bar{\Omega})$ implies that $\hat{K}_k \to 0$ as $k \to \infty$. See [22, Chapter 1, Section 4.3]. We have that K_c is a compact operator on a Banach space [32, Theorem 8.3]. Therefore, the spectrum of K_c contains only the eigenvalues $\hat{K}_k$ and its limit point 0 [1, Theorem 7.3]. If we fix ϵ, observe that part (3) follows using the same reasoning of parts (1) and (2) since $J \in C^1(\bar{\Omega})$ and J_c is also compact. □

In what follows, we will use the fact that the spectra of $K_c - \hat{K}_0$ and $J_c - \hat{J}_0$ are just shifted versions of the spectra in the above lemma.

Assumption 2.11. (Smoothness of the nonlinearity and a homogeneous equilibrium). Let $\chi \in \mathbb{N}$ be arbitrary. Assume that $f, g : \mathbb{R}^2 \to \mathbb{R}$ are $C^{1+\chi}$-functions, and that there exists a point $(\bar{u}_0, \bar{v}_0) \in \mathbb{R}^2$ with $f(\bar{u}_0, \bar{v}_0) = g(\bar{u}_0, \bar{v}_0) = 0$. That is, $(\bar{u}_0, \bar{v}_0)$ is a homogeneous equilibrium for System (1.1). If $\chi \geq 2$, assume further that the partial derivatives of f and g of order $2, 3, \ldots, \chi$ at the $(\bar{u}_0, \bar{v}_0)$ vanish.

Assumption 2.12 (Turing instability)**.** Assume that f and g satisfy the smoothness conditions of Assumption 2.11 and that the homogeneous equilibrium of System (1.1) exhibits Turing instability. That is, in the absence of nonlocal and local diffusion terms, the homogeneous equilibrium is stable, but in the presence of the nonlocal and local diffusion terms, it is unstable.

Lemma 2.13 (Turing Instability Conditions)**.** *The homogeneous equilibrium of System* (1.1) *exhibits Turing instability. This is true if and only there exists $d > 0$ be such that*

(1) $f_u + g_v < 0$,
(2) $f_u g_v - f_v g_u > 0$,
(3) $df_u + g_v > 0$,
(4) $(df_u + g_v)^2 - 4d(f_u g_v - f_v g_u) > 0$,

where the partials are evaluated at the homogeneous equilibrium $(\bar{u}_0, \bar{v}_0)$.

For a proof of the above lemma, see [27]. In particular, the first two conditions in this lemma ensure the stability of the homogeneous equilibrium in the absence of diffusion. The next two conditions ensure that the homogeneous equilibrium is unstable when diffusion is present. Note that the first and third conditions show that $d > 1$.

Assumption 2.14 (Real eigenvalues for the nonlinearity)**.** Suppose that f and g satisfy Assumption 2.11. Assume that the eigenvalues of the linearization are real.

This section is concluded with definitions of the function spaces that provide the context for the results of this chapter.

Definition 2.15 (Function Spaces)**.** Let $L^2_{\text{per}}(\Omega)$ be the space of smoothly periodic functions on Ω that belong to $L^2(\Omega)$ as defined by Definition 2.2. Let

$$\mathbb{L}^2_{\text{per}}(\Omega) = L^2_{\text{per}}(\Omega) \times L^2_{\text{per}}(\Omega). \tag{2.7}$$

For $s > 0$, let $H^s(\Omega)$ be the standard fractional Sobolev space for real-valued functions and let $H^s_{\text{per}}(\Omega)$ be the space of periodic functions in $H^s_{\text{per}}(\Omega)$. Let

$$\mathbb{H}^s_{\text{per}}(\Omega) = H^s_{\text{per}}(\Omega) \times H^s_{\text{per}}(\Omega). \tag{2.8}$$

3. Properties of the linearization

In this section, we state and derive explicit representations for the eigenvalues and eigenfunctions of the linearized right hand side of System (1.1). For $0 < \beta \leq 1$ and $0 \leq \theta < 1$, we show that if Assumptions 2.1 - 2.14 are satisfied, then there exists an ϵ_0 such that for $0 < \epsilon \leq \epsilon_0$, the homogeneous equilibrium will be unstable.

The following system is the linearized form of System (1.1):

$$U' = D\mathcal{J}_\epsilon U + BU, \tag{3.1}$$

where

$$D = \begin{pmatrix} 1 & 0 \\ 0 & d \end{pmatrix}, \tag{3.2}$$

$$\mathcal{J}_\epsilon = \epsilon\mathcal{J}_1 + \epsilon^{1-\theta}\mathcal{J}_2 \tag{3.3}$$

$$\mathcal{J}_1 = \beta \begin{pmatrix} \Delta & 0 \\ 0 & \Delta \end{pmatrix} \tag{3.4}$$

$$\mathcal{J}_2 = (1-\beta)\epsilon^\theta \begin{pmatrix} J_c - \hat{J}_0 & 0 \\ 0 & J_c - \hat{J}_0 \end{pmatrix}, \tag{3.5}$$

$$B = \begin{pmatrix} f_u(\bar{u}_0, \bar{v}_0) & f_v(\bar{u}_0, \bar{v}_0) \\ g_u(\bar{u}_0, \bar{v}_0) & g_v(\bar{u}_0, \bar{v}_0) \end{pmatrix}, \tag{3.6}$$

for $U = (u, v)^T$. For the sake of notation, we shall denote this operator as

$$\mathcal{H}_\epsilon = D\mathcal{J}_\epsilon + B, \tag{3.7}$$

where $\mathcal{H}_\epsilon : \mathbb{L}^2_{\text{per}}(\Omega) \to \mathbb{L}^2_{\text{per}}(\Omega)$. The domains for the local and nonlocal operators are given respectively as $D(\Delta) = H^2_{\text{per}}(\Omega)$ and $D(J_c) = L^2_{\text{per}}(\Omega)$. Thus, for $0 < \beta \leq 1$, the domain of $\mathcal{H}_\epsilon$ is given as $D(\mathcal{H}_\epsilon) = \mathbb{H}^2_{\text{per}}(\Omega)$ and for $\beta = 0$, $D(\mathcal{H}_\epsilon) = \mathbb{L}^2_{\text{per}}(\Omega)$.

The asymptotic growth of the eigenvalues of the negative Laplacian and J_c is important for our results. Since both the negative Laplacian and J_c have the same set of eigenfunctions, the eigenvalues of $-\beta\Delta - (1-\beta)(J_c - \hat{J}_0)$ are given as

$$\nu_{k,\epsilon} = \beta\kappa_k + (1-\beta)(\hat{J}_0 - \hat{J}_k), \tag{3.8}$$

where $k \in \mathbb{N}$. Here, the κ_k are the eigenvalues of $-\Delta$ as defined in Definition 2.2 and the $\hat{J}_k$ are the eigenvalues of J_c as defined by Equation 2.2. Note that $\nu_{k,\epsilon}$ is real since κ_k and $\hat{J}_k$ are real. For rectangular domains, the growth of eigenvalues of the negative Laplacian are given as

$$\lim_{k\to\infty} \frac{\kappa_k}{k^{2/n}} = C_\Omega, \tag{3.9}$$

where $n = \dim\,\Omega$ and $0 < C_\Omega < \infty$ [10]. Since $J \in C^1(\bar{\Omega})$, by Lemma 2.10, $\lim_{k\to\infty}(\hat{J}_0 - \hat{J}_k) = \hat{J}_0$. Thus, we see that for fixed ϵ, if $\beta > 0$,

$$\lim_{k\to\infty} \frac{\nu_{k,\epsilon}}{k^{2/n}} = \beta \cdot C_\Omega, \tag{3.10}$$

whereas if $\beta = 0$, $\lim_{k\to\infty} \nu_{k,\epsilon} = \hat{J}_0$. Note that $\hat{J}_0$ depends on ϵ.

Lemma 3.1 (Eigenvalues of $\mathcal{H}_\epsilon$)**.** *Suppose that Assumptions 2.1 - 2.14 are satisfied. The eigenvalues of $\mathcal{H}_\epsilon$ are*

$$\lambda^\pm_{k,\epsilon} = \lambda^\pm(\epsilon\nu_{k,\epsilon}) = \frac{b(\epsilon\nu_{k,\epsilon}) \pm \sqrt{(b(\epsilon\nu_{k,\epsilon})^2 - 4c(\epsilon\nu_{k,\epsilon})}}{2}, \tag{3.11}$$

where $\lambda^{\pm}_{k,\epsilon} \in \mathbb{R}$ *and*

$$b(s) = (f_u + g_v) - (d+1)s \tag{3.12}$$

$$c(s) = (f_u g_v - g_u f_v) - (df_u + g_v)s + ds^2, \tag{3.13}$$

and $\nu_{k,\epsilon}$ *are the eigenvalues of* $-\beta\Delta - (1-\beta)(J_c - \hat{J}_0)$ *associated with* $\lambda^{\pm}_{k,\epsilon}$. *The normalized eigenfunctions of* $\mathcal{H}_\epsilon$ *are given as* $\Psi^{\pm}_{k,\epsilon} = E^{\pm}(\epsilon\nu_{k,\epsilon})\cdot\psi_k$, *where* $E^{\pm}(\epsilon\nu_{k,\epsilon})$ *are eigenfunctions of* $B - \epsilon\nu_{k,\epsilon}D$. *If* $\beta = 0$, *then for each fixed* ϵ, $\lambda^{\pm}(\epsilon\cdot\nu_{k,\epsilon}) \to \lambda^{\pm}(\epsilon\cdot\hat{J}_0)$ *as* $k \to \infty$.

Proof. Fix $\epsilon > 0$. We begin by showing that any eigenvalue of $\mathcal{H}_\epsilon$ is expressible as $\lambda^{\pm}_{k,\epsilon}$ for some k. Let λ and U be an eigenvalue and corresponding eigenfunction of $\mathcal{H}_\epsilon$, respectively, where $U \in \mathbb{L}^2_{\text{per}}(\Omega)$ and $U \neq (0,0)$. We can write $U \in \mathbb{L}^2_{\text{per}}(\Omega)$ as

$$U = \sum_{j=0}^{\infty} \psi_j r_j,$$

where $r_j = (s_j, t_j)^T$ and $s_j, t_j \in \mathbb{R}$. Since U is nontrivial, then for $j = k$, $r_j \neq (0,0)^T$. Since λ is an eigenvalue of $\mathcal{H}_\epsilon$, and U is the corresponding eigenfunction,

$$\mathcal{H}_\epsilon U - \lambda U = 0.$$

Using 3.7, we evaluate the left hand side as

$$\mathcal{H}_\epsilon U - \lambda U = \sum_{j=0}^{\infty}(D\mathcal{J}_\epsilon + B - \lambda I)\psi_j r_j = \sum_{j=0}^{\infty}(-\epsilon\nu_{j,\epsilon}D + B - \lambda I)\psi_j r_j.$$

Since the ψ_j are linearly independent,

$$(-\epsilon\nu_{j,\epsilon}D + B - \lambda I)r_j = 0,$$

for all j. For $j = k$, we see that r_k is nontrivial, which implies that $-\epsilon\nu_{k,\epsilon}D + B - \lambda I$ must be singular for some k. Therefore, we have that

$$|-\epsilon\nu_{k,\epsilon}D + B - \lambda I| = 0.$$

Solving for λ gives the result.

Let $\lambda^{\pm}_{k,\epsilon}$ be as given by Equation 3.11 and $E^{\pm}(\epsilon\nu_{k,\epsilon})$ be the associated eigenfunction of $B - \epsilon\nu_{k,\epsilon}D$. To show that $\lambda^{\pm}_{k,\epsilon}$ is an eigenvalue of $\mathcal{H}_\epsilon$ and $\Psi^{\pm}_{k,\epsilon}$ is an eigenvector of $\mathcal{H}_\epsilon$, we compute

$$\begin{aligned}\mathcal{H}_\epsilon\Psi^{\pm}_{k,\epsilon} &= D\mathcal{J}_\epsilon\Psi^{\pm}_{k,\epsilon} + B\Psi^{\pm}_{k,\epsilon}\\ &= \lambda^{\pm}_{k,\epsilon}E^{\pm}(\epsilon\nu_{k,\epsilon})\psi_k\\ &= \lambda^{\pm}_{k,\epsilon}\Psi^{\pm}_{k,\epsilon}\end{aligned}$$

Since the $\lambda^{\pm}_{k,\epsilon}$ are distinct and the algebraic multiplicity is 1, the geometric multiplicity is also 1. Thus, each eigenvalue corresponds to one and only one eigenfunction. As $k \to \infty$, Lemma 2.10 shows that $\hat{J}_k \to 0$. If $\beta = 0$, $\lambda^{\pm}(\epsilon\nu_{k,\epsilon}) \to \lambda^{\pm}(\epsilon\hat{J}_0)$ as $k \to \infty$. Assumption 2.14 implies that $\lambda^{\pm}_{k,\epsilon} \in \mathbb{R}$. □

We now give a useful, sufficient condition that describes when the eigenvalues of the linearization are real.

Lemma 3.2. *Suppose that Assumptions 2.1 - 2.13 are satisfied. A sufficient condition on f and g for the eigenvalues of our system to be real:*

$$(f_u + g_v)^2 - 4(f_u g_v - f_v g_u) > 0.$$

Proof. Suppose that $(f_u+g_v)^2-4(f_u g_v-f_v g_u) > 0$. Using Equations (3.11), (3.12) and (3.13), we see that the eigenvalues are real if and only if $b^2(s) - 4c(s) \geq 0$, for which $s = \epsilon\nu_{k,\epsilon} > 0$. Expanding the left hand side of the inequality, we have

$$b^2(s)-4c(s) = (f_u+g_v)^2-4(f_u g_v-f_v g_u)+(d-1)^2 s^2-2(d+1)(f_u+g_v)s+4(df_u+g_v)s.$$

For the Turing instability conditions in Lemma (2.13), we have

$$(d-1)^2 s^2 - 2(d+1)(f_u + g_v)s + 4(df_u + g_v)s \geq 0.$$

Thus, the eigenvalues are real. □

Figure 7 shows eigenvalues $\lambda^{\pm}_{k,\epsilon}$ for fixed $\beta = 0$ and $0 \leq \theta < 1$. In particular, as $\epsilon \to 0$, $\lim_{k\to\infty} \nu_{k,\epsilon} = 0$. The convergence to 0 becoming slower as $\theta \to 1$, and the expression does not converge to zero for $\theta = 1$. In contrast, for all $\beta > 0$ and $0 \leq \theta \leq 1$, $\nu_{k,\epsilon}$ limit to ∞ for $k \to \infty$. Thus for $0 \leq \theta < 1$, the eigenvalues of the mixed diffusion operator as $\epsilon \to 0$ have the property that $\epsilon\nu_{k,\epsilon}$ behave asymptotically like $\epsilon\kappa_k$ for $0 < \beta \leq 1$.

In the following lemma, we analyze the behavior of the eigenvalues $\lambda^{\pm}_{k,\epsilon} = \lambda(\epsilon\nu_{k,\epsilon})$ by replacing $\epsilon\nu_{k,\epsilon}$ in Eqn. 3.11 with the continuous real variable s.

Lemma 3.3. *Under Assumptions 2.12 and 2.14, the following properties of $\lambda^{\pm}(s)$ are true for $s \geq 0$:*

- $\lambda^-(s) < \lambda^+(s)$.
- $\lambda^+(0) < 0$.
- $\lambda^+(s)$ *has a unique maximum* $\lambda^+_{\max}$.
- $\lambda^+(s)$ *has two real roots,* s_ℓ *and* s_r.
- $\lambda^-(s)$ *is strictly decreasing with* $\lambda^-(s) < 0$.
- $\lim_{s\to\infty}(\lambda^+(s)/s) = -1$.
- $\lim_{s\to\infty}(\lambda^-(s)/s) = -d$.

Proof. The proof follows exactly as that given in [33, Lemma 3.4]. Application of Inequalities (1), (3) of Lemma 2.13 and Assumption 2.14 give that $b(s)^2 - 4c(s) > 0$ for every $s \geq 0$. Part (1) of Lemma 2.13 shows that $b(s) < 0$ for all $s \geq 0$, and therefore, $\lambda^-(s) < 0$. Consequently, we have that $\lambda^-(s) < \lambda^+(s)$ for all $s \geq 0$. We also have that $\lambda^+(0) < 0$. For $\lambda^+(s) > 0$, then $c(s) < 0$. Parts (2) – (4) of Lemma 2.13 show that $c(s) < 0$ is equivalent to $s_\ell < s < s_r$, where

$$s_{l/r} = \frac{1}{2d}\left((df_u + g_v) \mp \sqrt{(df_u + g_v)^2 - 4d(f_u g_v - f_v g_u)}\right). \tag{3.14}$$

Since λ^+ is continuous on $[s_\ell, s_r]$, it achieves a maximum value, denoted as $\lambda^+_{\max}$. Computing the asymptotic limits for $\lambda^{\pm}(s)/s$ gives the final part of the lemma. □

Lemma 3.4. *Suppose that Assumptions 2.1 - 2.14 are satisfied. For $0 \leq \beta \leq 1$, the eigenfunctions of $\mathcal{H}_\epsilon$ form a complete set for $\mathbb{X}$. The angle between $E^{\pm}_{k,\epsilon}$ is bounded away from π and 0.*

Proof. The eigenfunctions are given by $\Psi^{\pm}_{k,\epsilon} = E^{\pm}_{k,\epsilon} \cdot \psi_k$, where $E^{\pm}_{k,\epsilon} = E^{\pm}(\epsilon \cdot \nu_{k,\epsilon})$ and $E^{\pm}(\cdot)$ is defined by Lemma 3.1. By Lemma 3.3, we see that for each $s \geq 0$, $\lambda^+(s) < \lambda^-(s)$. Thus, the eigenvectors $E^{\pm}(s)$ are linearly independent for all $s \geq 0$.

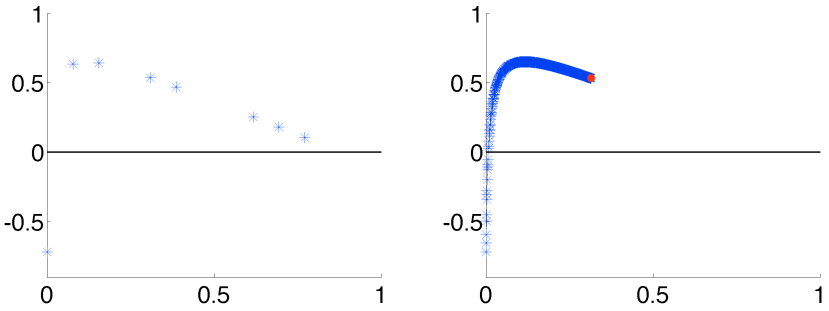

(a) Large ϵ

(b) Medium ϵ

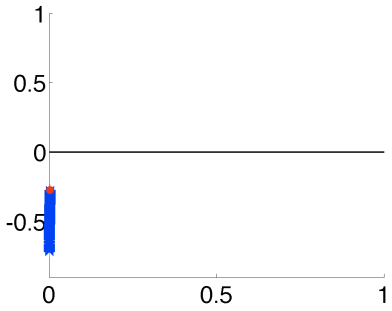

(c) Small ϵ

FIGURE 7. The eigenvalue dispersion curve for System (1.1), $\beta = 0$. This figure shows a plot of the eigenvalues $\lambda^+(\epsilon\nu_{k,\epsilon})$ versus $\nu_{k,\epsilon}$, where the $\nu_{k,\epsilon}$ are the eigenvalues of the nonlocal diffusion operator. Parameters ϵ and $0 \le \theta < 1$, are fixed (with θ defined in Assumption 2.4). The points are plotted as black asterisks, and $(\hat{J}_0, \lambda^+(\epsilon\hat{J}_0))$ is given as a red asterisk. In Part (a), the eigenvalues are sparsely distributed on the curve when ϵ is large. In Part (b), as ϵ decreases, the eigenvalues are more closely spaced. Since $\beta = 0$, the plotted points limit on the point $(\hat{J}_0, \lambda^+(\epsilon \cdot \hat{J}_0))$. As $\epsilon \to 0$ in Subfigure (c), the eigenvalues lie on the leftmost part of the curve where all of the eigenvalues are negative.

However, we are only interested in the discrete points of s in which $s = \epsilon \cdot \nu_{k,\epsilon}$. All that is left to show is that $\epsilon \cdot \nu_{k,\epsilon} \ge 0$ for all $k \ge 0$. By Assumption 2.4, $\epsilon(1-\beta)(\hat{J}_0 - \hat{J}_k) \ge 0$ for $0 \le \beta \le 1$. Definition 2.2 shows that $\kappa_k \ge 0$ for all $k \ge 0$. Since $\nu_{k,\epsilon} = \beta\kappa_k + (1-\beta)(\hat{J}_0 - \hat{J}_k) \ge 0$, we have shown the first part of this lemma. The $\Psi^{\pm}_{k,\epsilon}$ form a complete set in $\mathbb{X}$ since the ψ_k form a complete set for $L^2(\Omega)$ and the $E^{\pm}_{k,\epsilon}$ are linearly independent.

For $\beta = 0$, fix $\epsilon_0 > 0$. As $k \to \infty$, we have that $\epsilon_0\nu_{k,\epsilon_0} \to \epsilon_0\hat{J}_0 < \infty$. Thus, all ν_{k,ϵ_0} are contained in some compact interval $[0, s_r^*]$. Since $0 \le \theta \le 1$, clearly $\epsilon\nu_{k,\epsilon} \in [0, s_r^*]$ for all $0 < \epsilon \le \epsilon_0$. Since the eigenvectors $E^{\pm}_{k,\epsilon}$ are linearly independent and the angle between the $E^{\pm}_{k,\epsilon}$ is bounded away from 0 and π. For $\beta > 0$, we need

to consider the limit as $s \to \infty$. The eigenfunctions of $B - sD$ are the same as $s^{-1}B - D$, and we see that as $s \to \infty$, $s^{-1}B - D$ approaches a diagonal matrix. Hence, the eigenfunctions become orthogonal as $s \to \infty$ and are bounded away from 0 and π. □

Lemma 3.5. *Suppose that Assumptions 2.4, 2.12 and 2.14 are satisfied. For $0 < \beta \leq 1$, there exists $\epsilon_0 > 0$, such that for all $\epsilon \leq \epsilon_0$, the homogeneous equilibrium of System* (1.1) *is unstable.*

Proof. The details follow the proof given in [33, Lemma 5.1]. Let $0 < \beta \leq 1$, $0 \leq \theta < 1$, and choose $0 < c_1 < c_2 < \lambda^+_{\max}$, where $\lambda^+_{\max}$ is given in Lemma 3.3. By Lemma 3.3 and Lemma 3.4, there exists a set of two compact intervals, which we call I, such that $\lambda^+_{k,\epsilon} \in [c_1, c_2]$ if and only if $\epsilon \cdot \nu_{k,\epsilon} \in I$. Using the asymptotic distribution of eigenvalues $\nu_{k,\epsilon}$ given in (3.10), we see that as $\epsilon \to 0$, the number of eigenvalues of $\mathcal{H}_\epsilon$ in $[c_1, c_2]$ is of the order $\epsilon^{-\dim\Omega/2}$. Thus, for some ϵ_0, we have that the homogeneous equilibrium is unstable for $0 < \epsilon \leq \epsilon_0$. □

Note that the estimates in the proof of the above lemma are more delicate for $\beta = 0$ with $\theta = 1$. Namely, the eigenvalues are discretely spaced along a continuous dispersion curve, meaning that even if the dispersion curve goes above zero, if the spacing of the eigenvalues is too large along the curve it is possible to miss the unstable region altogether, resulting in no unstable eigenvalues. The result is never true for $\beta = 0$, with $0 \leq \theta < 1$ (cf. Fig. 7.)

3.1. **Spectrum of the linear operator.** The results presented in the following sections depend upon the spectrum of $\mathcal{H}_\epsilon$ and its associated spectral gaps. For this reason, we describe the full spectrum of $\mathcal{H}_\epsilon$ for all $0 \leq \beta \leq 1$. We begin with a theorem describing the spectrum of $\mathcal{H}_\epsilon$, followed by useful lemmas used in proving the theorem and finally the proof.

Theorem 3.6 (Spectrum of $\mathcal{H}_\epsilon$)**.** *Suppose that Assumptions 2.1 - 2.14 are satisfied. Let $\mathcal{H}_\epsilon$ be as defined in* (3.7)*. If $0 < \beta \leq 1$, the spectrum contains only the eigenvalues of $\mathcal{H}_\epsilon$. If $\beta = 0$, then the spectrum of $\mathcal{H}_\epsilon$ consists of the eigenvalues $\mathcal{H}_\epsilon$ and the points $\lambda^\pm(\epsilon\hat{J}_0)$.*

We introduce a norm that will be useful for the spectrum computation. As we show in the next lemma, the equivalence of the $\mathbb{L}^2$-norm and this new norm is possible since the angle between the $E^\pm_{k,\epsilon}$ is bounded away from both 0 and π.

Definition 3.7. Let $\epsilon > 0$. For $U \in \mathbb{L}^2_{\text{per}}(\Omega)$, Lemma 3.4 implies that U may be written as

$$U = \sum_{k=0}^{\infty} \left((\alpha^+_{k,\epsilon}) E^+_{k,\epsilon} + (\alpha^-_{k,\epsilon}) E^-_{k,\epsilon} \right) \cdot \psi_k. \tag{3.15}$$

When the following is finite, define the $\|\cdot\|_{\#}-$norm as

$$\|U\|^2_{\#} = \sum_{k=0}^{\infty} \left((\alpha^+_{k,\epsilon})^2 + (\alpha^-_{k,\epsilon})^2 \right). \tag{3.16}$$

Lemma 3.8. *Suppose that Assumptions 2.1 - 2.14 are satisfied. Let $\|\cdot\|_{\#}$ be as defined in Definition 3.7. For $U \in \mathbb{L}^2_{\text{per}}(\Omega)$,*

$$\sqrt{1-r}\|U\|_{\#} \leq \|U\|_{\mathbb{L}^2_{\text{per}}(\Omega)} \leq \sqrt{1+r}\|U\|_{\#},$$

where $|(E^+_{k,\epsilon}, E^-_{k,\epsilon})_{\mathbb{R}^2}| \le r < 1$ *for all* $k \in \mathbb{Z}$.

Proof. Let $\epsilon > 0$. For $U \in \mathbb{L}^2_{\rm per}(\Omega)$, we write U as

$$U = \sum_{k=0}^{\infty} \left((\alpha^+_{k,\epsilon}) E^+_{k,\epsilon} + (\alpha^-_{k,\epsilon}) E^-_{k,\epsilon} \right) \cdot \psi_k.$$

Note that r exists by Lemma 3.4. Computing the square of the $\mathbb{L}^2_{\rm per}(\Omega)$-norm of U yields

$$\begin{aligned}
\|U\|^2_{\mathbb{L}^2_{\rm per}(\Omega)} &= \sum_{k=0}^{\infty} ((\alpha^+_{k,\epsilon})^2 + (\alpha^-_{k,\epsilon})^2 + 2\alpha^+_{k,\epsilon}\alpha^-_{k,\epsilon}(E^+_{k,\epsilon}, E^-_{k,\epsilon})), \\
&\le \sum_{k=0}^{\infty} ((\alpha^+_{k,\epsilon})^2 + (\alpha^-_{k,\epsilon})^2) + 2|\alpha^+_{k,\epsilon}\alpha^-_{k,\epsilon}| r, \\
&\le \sum_{k=0}^{\infty} (\alpha^+_{k,\epsilon})^2 + (\alpha^-_{k,\epsilon})^2 + r((\alpha^+_{k,\epsilon})^2 + (\alpha^-_{k,\epsilon})^2) \\
&= (1+r) \sum_{k=0}^{\infty} (\alpha^+_{k,\epsilon})^2 + (\alpha^-_{k,\epsilon})^2, \\
&= (1+r)\|U\|^2_{\#}.
\end{aligned}$$

Taking square roots gives the right hand inequality. For the other direction, we compute

$$\begin{aligned}
\|U\|^2_{\mathbb{L}^2(\Omega)} &\ge \sum_{k=0}^{\infty} (\alpha^+_{k,\epsilon})^2 + (\alpha^-_{k,\epsilon})^2 - \left((\alpha^+_{k,\epsilon})^2 + (\alpha^-_{k,\epsilon})^2 \right) (E^+_{k,\epsilon}, E^-_{k,\epsilon})), \\
&\ge (1-r)\|U\|^2_{\#}.
\end{aligned}$$

Again, taking square roots gives the left hand inequality. □

The following lemma allows us to describe the full spectrum of $\mathcal{H}_\epsilon$ for $\beta = 0$.

Lemma 3.9 (Adjoint of $\mathcal{H}_\epsilon$)**.** *Suppose that Assumptions 2.1 - 2.4 are satisfied and* $\beta = 0$. *Let* $\mathcal{H}_\epsilon$ *be as defined in* (3.7) *and* $\mathcal{J}_2$ *be as defined in* (3.5). *The adjoint of* $\mathcal{H}_\epsilon$ *is given as* $\mathcal{H}^*_\epsilon = \epsilon^{1-\theta} D\mathcal{A} + B^T$, *where*

$$\mathcal{A} = \begin{pmatrix} A^J_c - \hat{J}_0 & 0 \\ 0 & A^J_c - \hat{J}_0 \end{pmatrix},$$

and A^J_c *is as defined in* (2.6). *If the periodic extension of* J *satisfies Assumption 2.8, then the adjoint of* $\mathcal{H}_\epsilon$ *is given as* $\mathcal{H}^*_\epsilon = \epsilon^{1-\theta} D\mathcal{J}_2 + B^T$.

Proof. Let $\epsilon > 0$. Application of Lemma 2.6 shows that the adjoint of $\epsilon^{1-\theta} D\mathcal{J}_2$ is $\epsilon^{1-\theta} D\mathcal{A}$. Since the adjoint of B is B^T, the adjoint of $\mathcal{H}_\epsilon$ is given as $\mathcal{H}^*_\epsilon = \epsilon D\mathcal{A} + B^T$. On the other hand if $J_{\rm per}$ satisfies Assumption 2.8, then J_c is self-adjoint by Lemma 2.6 and the adjoint of $\mathcal{H}_\epsilon$ is given as $\mathcal{H}^*_\epsilon = \epsilon^{1-\theta} D\mathcal{J}_2 + B^T$. □

We are now ready to prove Theorem 3.6 that describes the full spectrum of $\mathcal{H}_\epsilon$ for all $0 \le \beta \le 1$.

Proof of Theorem 3.6. Let $0 < \beta \le 1$. Recall that $\mathcal{J}_\epsilon = \epsilon \mathcal{J}_1 + \epsilon^{1-\theta} \mathcal{J}_2$ as defined in Equations (3.3) - (3.5). Since $\epsilon D\mathcal{J}_1 + B$ has a compact resolvent, its spectrum contains only eigenvalues [31]. The operator $D\mathcal{J}_\epsilon + B$ also has a compact resolvent,

since $\epsilon D\mathcal{J}_1 + B$ has a compact resolvent and $\epsilon^{1-\theta}D\mathcal{J}_2$ is a bounded operator. See [12, pg. 120]. Since the resolvent is compact, then for $0 < \beta \leq 1$, the spectrum of $\mathcal{H}_\epsilon$ contains only eigenvalues [21, pg. 187]. We now focus on the case $\beta = 0$.

In [20], a sufficient condition is given that states for certain self-adjoint operators defined on Hilbert spaces, all points of the spectrum are expressible as limit points of eigenvalues. The remainder of the proof shows that in general, it is not necessary for an operator to be self-adjoint.

A value λ is in the spectrum of $\mathcal{H}_\epsilon$ is either in the point spectrum, continuous spectrum or residual spectrum. We have already computed the eigenvalues of $\mathcal{H}_\epsilon$, which implies that the point spectrum of $\mathcal{H}_\epsilon$ is nonempty. We now show that the residual spectrum must be empty. Since $\mathcal{J}$ is self-adjoint, then by similar reasoning used in the proof of the eigenvalues of $\mathcal{H}_\epsilon$, we have that the eigenvalues of $\mathcal{H}_\epsilon^*$ are given as the roots of

$$\det(B^T - \epsilon(\hat{J}_0 - \hat{J}_k)D - \lambda_k^{*\pm} I) = 0. \tag{3.17}$$

Since the determinant of a matrix is the same as the determinant of the transpose of that matrix, we have

$$\det(B^T - \epsilon(\hat{J}_0 - \hat{J}_k)D - \lambda_k^{*\pm} I) = \det(B - \epsilon(\hat{J}_0 - \hat{J}_k)D - \lambda_k^{\pm} I). \tag{3.18}$$

Thus, the eigenvalues of $\mathcal{H}_\epsilon^*$ are the same as those of $\mathcal{H}_\epsilon$. By [34, Theorem 8.7.1], we see that if a point is in the residual spectrum of $\mathcal{H}_\epsilon$, then its conjugate must also be an eigenvalue of its adjoint operator. Since the eigenvalues for both $\mathcal{H}_\epsilon$ and $\mathcal{H}_\epsilon^*$ are the same, the residual spectrum of $\mathcal{H}_\epsilon$ must be empty.

The last portion of the spectrum to check is the continuous spectrum. We now show that both $\lambda^{\pm}(\epsilon\hat{J}_0)$ are contained in the continuous spectrum. The proof for $\lambda^{-}(\epsilon\hat{J}_0)$ follows in the same manner as the proof for $\lambda^{+}(\epsilon\hat{J}_0)$, so we only give proof for $\lambda^{+}(\epsilon\hat{J}_0)$. Consider $\lambda^{+}(\epsilon\hat{J}_0)I - \mathcal{H}_\epsilon$ and let $f_k = \Psi_{k,\epsilon}^{+}/\|\Psi_{k,\epsilon}^{+}\|_{\mathbb{L}^2_{\text{per}}(\Omega)}$ where the $\Psi_{k,\epsilon}^{+}$ are eigenfunctions of $\mathcal{H}_\epsilon$. Since $\lambda^{+}(\epsilon\hat{J}_0)$ is not an eigenvalue of $\mathcal{H}_\epsilon$, we have that $\lambda^{+}(\epsilon\hat{J}_0)I - \mathcal{H}_\epsilon$ is one-to-one. Thus,

$$\begin{aligned}\|(\lambda^{+}(\epsilon\hat{J}_0)I - \mathcal{H}_\epsilon)f_k\|_{\mathbb{L}^2_{\text{per}}(\Omega)} &= \|(\lambda^{+}(\epsilon\hat{J}_0) - \lambda_{k,\epsilon}^{+})f_k\|_{\mathbb{L}^2_{\text{per}}(\Omega)} \\ &\leq |\lambda^{+}(\epsilon\hat{J}_0) - \lambda_{k,\epsilon}^{+}|\end{aligned}$$

As $k \to \infty$, $\lambda_{k,\epsilon}^{+} \to \lambda^{+}(\epsilon\hat{J}_0)$ and

$$\|(\lambda^{+}(\epsilon\hat{J}_0)I - \mathcal{H}_\epsilon)f_k\|_{\mathbb{L}^2_{\text{per}}(\Omega)} \to 0.$$

Since $\|f_k\|_{\mathbb{L}^2_{\text{per}}(\Omega)} = 1$ for all k and $\|(\lambda^{+}(\epsilon\hat{J}_0)I - \mathcal{H}_\epsilon)f_k\|_{\mathbb{L}^2_{\text{per}}(\Omega)} \to 0$, we see that $(\lambda^{+}(\epsilon\hat{J}_0)I - \mathcal{H}_\epsilon)^{-1}$ is unbounded. Thus, $\lambda^{\pm}(\epsilon\hat{J}_0)$ is in the continuous spectrum of $\mathcal{H}_\epsilon$.

For the continuous spectrum, we have shown that the limit points of the eigenvalues are elements of this set. We now show that the points in the continuous spectrum must be limit points of the eigenvalues. To do this, we will argue by contradiction. Suppose that λ is in the continuous spectrum, but that it is not a limit point of eigenvalues of $\mathcal{H}_\epsilon$. Since the $\|\cdot\|_{\#}$ is equivalent to the $\mathbb{L}^2-$norm by Lemma 3.8, we have that for some sequence of $f_n \in \mathbb{L}^2_{\text{per}}(\Omega)$ with $\|f_n\|_{\#} = 1$ for all

n, $\|(\lambda I - \mathcal{H}_\epsilon)f_n\|_\# \to 0$ as $n \to \infty$. Since $f_n \in \mathbb{L}^2_{\text{per}}(\Omega)$, we can write f_n as

$$f_n = \sum_{k=0}^{\infty}((\alpha^+_{n,k,\epsilon})E^+_{k,\epsilon} + (\alpha^-_{n,k,\epsilon})E^-_{k,\epsilon}) \cdot \psi_k.$$

By definition of the continuous spectrum, λ can not be an eigenvalue. Since we assumed that it is also not a limit point of eigenvalues, there exists $M > 0$ such that $M \le |\lambda - \lambda^\pm_{k,\epsilon}|$ for all k. Thus

$$\begin{aligned}\|(\lambda I - \mathcal{H}_\epsilon)f_n\|^2_\# &= \sum_{k=0}^{\infty}(\lambda - \lambda^+_{k,\epsilon})^2(\alpha^+_{n,k,\epsilon})^2 + (\lambda - \lambda^-_{k,\epsilon})^2(\alpha^-_{n,k,\epsilon})^2,\\ &\ge M^2\sum_{k=0}^{\infty}((\alpha^+_{n,k,\epsilon})^2 + (\alpha^-_{n,k,\epsilon})^2),\\ &= M^2\|f_n\|^2_\# = M^2 > 0.\end{aligned}$$

However, this is a contradiction, since $\|(\lambda I - \mathcal{H}_\epsilon)f_n\|_\# \to 0$. Therefore, the continuous spectrum of $\mathcal{H}_\epsilon$ contains only $\lambda^\pm(\epsilon\hat{J}_0)$. □

4. Almost linear behavior

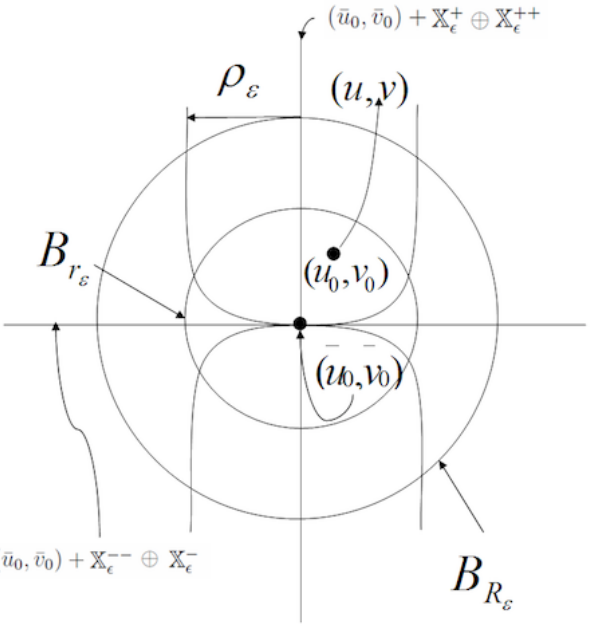

Figure 8. Schematic depicting early pattern formation as described in Theorem 4.8. The initial condition (u_0, v_0) of the solution (u, v) is within a parabolic region surrounding the unstable subspace spanned by the eigenfunctions of the most unstable eigenvalues. For most solutions with this type of initial conditions, the solutions remain close to the unstable space during the early stage of pattern formation.

To prove our main results, we use the abstract theory and techniques developed for the Cahn-Hilliard equation found in [25, 26]. The theory requires an abstract evolution equation of the form

$$U_t = \mathcal{H}_\epsilon U + F(U), \tag{4.1}$$

on some appropriate function space $\mathbb{X}$ that satisfies the following assumptions.

(H1) The operator $-\mathcal{H}_\epsilon$ is a sectorial operator on $\mathbb{X}$.

(H2) There exists a decomposition $\mathbb{X} = \mathbb{X}^{--} \oplus \mathbb{X}^{-} \oplus \mathbb{X}^{+} \oplus \mathbb{X}^{++}$, such that all of these subspaces are finite except $\mathbb{X}^{--}$, and such that the linear semigroup corresponding to $U_t = \mathcal{H}_\epsilon U$ satisfies several dichotomy estimates.

(H3) The nonlinearity $F : \mathbb{X}^\alpha \to \mathbb{X}$ is continuously differentiable, and satisfies both $F(\bar{u}_0, \bar{v}_0) = 0$ and $DF(\bar{u}_0, \bar{v}_0) = 0$.

In light of how $\mathcal{H}_\epsilon$ is defined in (3.7), we define the nonlinearity of the evolution equation given by 4.1 in the following way. Define the function $h : \mathbb{R}^2 \to \mathbb{R}^2$ to be the nonlinear part of (f, g) of System (1.1) in the following sense. Let

$$\hat{h}(u, v) = (f(u, v), g(u, v))$$

and

$$h(u, v) = \hat{h}(u, v) - \hat{h}_u(\bar{u}_0, \bar{v}_0) \cdot (u - \bar{u}_0) - \hat{h}_v(\bar{u}_0, \bar{v}_0) \cdot (v - \bar{v}_0). \tag{4.2}$$

Setting

$$F(U) = h(u, v) \quad \text{for } U = (u, v) \tag{4.3}$$

gives the nonlinear portion of (4.1).

Lemma 4.1. *For System* (1.1)*, suppose that Assumptions 2.1 - 2.14 are satisfied and that* $0 < \beta \leq 1$*. Let* $\mathcal{H}_\epsilon$ *be as defined in* (3.7)*.* $\mathcal{H}_\epsilon$ *is a sectorial operator.*

Proof. For $0 < \beta \leq 1$, again we note that the operator $\epsilon^{1-\theta} D\mathcal{J}_2$ is a bounded perturbation of $\epsilon D\mathcal{J}_1 + B$, which is a sectorial operator [18]. Thus, $\mathcal{H}_\epsilon$ is sectorial [31, 17]. □

An important aspect of our analysis depends upon how the eigenfunctions of $\mathcal{H}_\epsilon$ populate the unstable subspaces as $\epsilon \to 0$. Note that the eigenvalues of $\mathcal{H}_\epsilon$ move arbitrarily close to $\lambda^+(\epsilon^{1-\theta} \cdot (1-\beta) \cdot \hat{K}_0)$ as $\epsilon \to 0$. The position of $\epsilon^{1-\theta} \cdot (1-\beta) \cdot \hat{K}_0$ relative to the unstable interval $[s_l, s_r]$ is important for the following reasons. For $\beta = 0$, if $\epsilon^{1-\theta} \cdot \hat{K}_0$ is too far to the right of s_r, then the nonlocal operator is stable. Furthermore, if $\theta = 1$, and $s_\ell < (1-\beta) \cdot \hat{K}_0 < s_r$, then there is a clustering of eigenvalues in the unstable interval as $\epsilon \to 0$. The following two assumptions exclude these cases.

Assumption 4.2. Suppose that $\hat{K}_0 > s_r$ such that only a finite nonzero number of the $\hat{K}_0 - \hat{K}_k$ are contained within the unstable interval $[s_\ell, s_r]$.

Assumption 4.3. For β satisfying $0 < \beta \leq 1$, $\hat{K}_0$ satisfies

$$\epsilon^{1-\theta}(1-\beta)\hat{K}_0 < s_\ell$$

as $\epsilon \to 0$.

We now provide a description of the decomposition of the phase space using the spectral gaps of $\mathcal{H}_\epsilon$. Select the following constants

$$\underline{c}^{--} < \bar{c}^{--} \ll 0 \ll \underline{c}^{-} < \bar{c}^{-} < \underline{c}^{+} < \bar{c}^{+} < \lambda^+_{\max}, \tag{4.4}$$

such that $\bar{c}^{--} - \underline{c}^{--}$, $\bar{c}^{-} - \underline{c}^{-}$, and $\bar{c}^{+} - \underline{c}^{+}$ are small. With Assumptions 4.2 - 4.3, the proofs of [33, Lemma 5.1,Corollary 5.2] show the existence of the intervals

$$J_\epsilon^{--} = [a_\epsilon^{--}, b_\epsilon^{--}] \subset [\underline{c}^{--}, \bar{c}^{--}], \tag{4.5}$$

$$J_\epsilon^{-} = [a_\epsilon^{-}, b_\epsilon^{-}] \subset [\underline{c}^{-}, \bar{c}^{-}], \tag{4.6}$$

$$J_\epsilon^{+} = [a_\epsilon^{+}, b_\epsilon^{+}] \subset [\underline{c}^{+}, \bar{c}^{+}], \tag{4.7}$$

where J_ϵ^{--}, J_ϵ^{-}, and J_ϵ^{+} are contained in the resolvent of $\mathcal{H}_\epsilon$ for sufficiently small ϵ. Furthermore, the length of each of these intervals is at least

$$d\epsilon^{\dim \Omega/2} \tag{4.8}$$

for some $\epsilon-$independent constant $d > 0$.

Definition 4.4 (Decomposition of the phase space)**.** Consider the intervals as defined by (4.5) - (4.7). Define the intervals $I_\epsilon^{--} = (-\infty, a_\epsilon^{--})$, $I_\epsilon^{-} = (b_\epsilon^{--}, a_\epsilon^{-})$, $I_\epsilon^{+} = (b_\epsilon^{-}, a_\epsilon^{+})$ and $I_\epsilon^{++} = (b_\epsilon^{+}, \lambda_{\max}^{+}]$. Denote $\mathbb{X}_\epsilon^{-}$, $\mathbb{X}_\epsilon^{+}$, $\mathbb{X}_\epsilon^{++}$ as the span of the eigenfunctions whose eigenvalues belong to I_ϵ^{-}, I_ϵ^{+}, and I_ϵ^{++}, respectively. Denote $\mathbb{X}_\epsilon^{--}$ as the orthogonal complement of the union of these three spaces (or equivalently, the space with Schauder basis I_ϵ^{--}).

The theory that we are applying makes use of fractional power spaces of $\mathcal{H}_\epsilon$. Let $a > \lambda_{\max}^{+}$. The fractional power spaces are given as $\mathbb{X}^\alpha = D((aI - \mathcal{H}_\epsilon)^\alpha)$ subject to the norm $\|U\|_\alpha = \|(aI - \mathcal{H}_\epsilon)^\alpha U\|_{\mathbb{L}^2(\Omega)}$ for $U \in \mathbb{X}^\alpha$. As pointed out in [17], the fractional power spaces of $\mathcal{H}_\epsilon$ are given as

$$\mathbb{X}^\alpha = \mathbb{H}_{\text{per}}^{2\alpha}(\Omega), \tag{4.9}$$

where $H_{\text{per}}^{2\alpha}(\Omega)$ are the Sobolev spaces of smoothly periodic functions on Ω and $0 < \alpha < 1$ as defined by Definition 2.15. By Lemma 3.4, $U \in \mathbb{L}_{\text{per}}^2(\Omega)$ is written as

$$U = \sum_{k=0}^{\infty} (\alpha_k^+ E_{k,\epsilon}^+ + \alpha_k^- E_{k,\epsilon}^-)\psi_k.$$

When the following is finite, define $\|\cdot\|_{**}$ as

$$\|U\|_{**}^2 = \sum_{k=0}^{\infty} (1+\kappa_k)^s \left((\alpha_k^+)^2 + (\alpha_k^-)^2\right). \tag{4.10}$$

Lemma 4.5. *Assume that Assumptions 2.1 and 2.11 are satisfied. The* $\|\cdot\|_{**}$*-norm given by* (4.10) *is equivalent to the* $\|\cdot\|_*$ *considered in* [33] *when restricted to* $\mathbb{L}_{\text{per}}^2(\Omega)$.

Proof. By [33, Lemma 4.2], $\|\cdot\|_*$ is equivalent to $\|\cdot\|_{\mathbb{H}^s(\Omega)}$. We now show equivalence of norms by showing that $\|\cdot\|_{**}$ is equivalent to the standard norm defined for $\mathbb{H}_{\text{per}}^s(\Omega)$. For $U \in \mathbb{L}_{\text{per}}^2(\Omega)$, we have that

$$\|U\|_{\mathbb{H}_{\text{per}}^s(\Omega)}^2 = \sum_{k=0}^{\infty} (1+\kappa_k)^s \|\alpha_k^+ \cdot E_{k,\epsilon}^+ + \alpha_k^- \cdot E_{k,\epsilon}^-\|_{\mathbb{R}^2}.$$

If we expand the terms in $\|\cdot\|_{\mathbb{R}^2}$, use Lemma 3.4 to note that the angle between $E_{k,\epsilon}^+$ and $E_{k,\epsilon}^-$ are bounded away from both 0 and π for all $k \in \mathbb{N}$ and $\epsilon > 0$, and apply the Cauchy-Schwarz lemma, we get the equivalence to the standard Sobolev norm. □

We have now established a suitable decomposition of the phase space. The following lemma gives dichotomy estimates, as well as estimates for critical quantities that we shall use for the first major result.

Lemma 4.6. *Assume that 2.1 - 2.14, 4.2 and 4.3 are satisfied and let $\mathcal{H}_\epsilon$ be as defined in* (3.7). *Let $S_\epsilon(t), t \geq 0$ denote the analytic semigroup on $\mathbb{X}$ generated by $\mathcal{H}_\epsilon$. Consider the decomposition as given by Definition 4.4 and let $\mathbb{X}^\alpha = \mathbb{H}^{2\alpha}_{\text{per}}(\Omega)$ be the fractional power spaces of $\mathcal{H}_\epsilon$.*

(a) *The spaces $\mathbb{X}^-_\epsilon$, $\mathbb{X}^+_\epsilon$, and $\mathbb{X}^{++}_\epsilon$ are finite-dimensional subspaces of $\mathbb{X}^\alpha$. Furthermore, all of the spaces introduced in Definition 4.4 are invariant under $S_\epsilon(t)$, and we denote the restrictions of the semigroup $S_\epsilon(t)$ to these spaces by the appropriate superscripts. The dimensions of these subspaces are proportional to $\epsilon^{-\dim\Omega/2}$.*

(b) *The following estimates are satisfied for arbitrary $U^{++} \in \mathbb{X}^{++}_\epsilon$, $U^+ \in \mathbb{X}^+_\epsilon$, $U^- \in \mathbb{X}^-_\epsilon$, and $U^{--}_{**} \in \mathbb{X}^{--}_\epsilon \cap \mathbb{X}^\alpha$:*

$$\begin{aligned}
\|S^{++}_\epsilon(t)U^{++}\|_{**} &\leq e^{b^+_\epsilon t}\cdot\|U^{++}\|_{**}, \quad \text{for } t \leq 0,\\
\|S^{+}_\epsilon(t)U^{+}\|_{**} &\leq e^{a^+_\epsilon t}\cdot\|U^{+}\|_{**}, \quad \text{for } t \geq 0,\\
\|S^{+}_\epsilon(t)U^{+}\|_{**} &\leq e^{b^-_\epsilon t}\cdot\|U^{+}\|_{**}, \quad \text{for } t \leq 0,\\
\|S^{-}_\epsilon(t)U^{-}\|_{**} &\leq e^{a^-_\epsilon t}\cdot\|U^{-}\|_{**}, \quad \text{for } t \geq 0,\\
\|S^{-}_\epsilon(t)U^{-}\|_{**} &\leq e^{b^{--}_\epsilon t}\cdot\|U^{-}\|_{**}, \quad \text{for } t \leq 0,\\
\|S^{--}_\epsilon(t)U^{--}_{**}\|_{**} &\leq e^{a^{--}_\epsilon t}\cdot\|U^{--}_{**}\|_{**}, \quad \text{for } t \geq 0,
\end{aligned}$$

There exists a constant $M^{--}_\epsilon > 0$ such that for $U^{--} \in \mathbb{X}^{--}_\epsilon$,

$$\|S^{--}_\epsilon(t)U^{--}\|_{**} \leq M^{--}_\epsilon \cdot t^{-\alpha}\cdot e^{a^{--}_\epsilon t}\cdot\|U^{--}\|_{\mathbb{L}^2(\Omega} \quad \text{for } t > 0. \tag{4.11}$$

where

$$M^{--}_\epsilon \leq C_1\cdot\epsilon^{-\alpha(2+\dim\Omega)/2} \quad \text{as } \epsilon \to 0.$$

(c) *There exists a constant $M_{\alpha,\epsilon} \geq 1$ which is proportional to $\epsilon^{-\alpha}$ as $\epsilon \to 0$, as well as an $\epsilon-$independent constant $C > 0$ such that for all $U \in \mathbb{X}^-_\epsilon \oplus \mathbb{X}^+_\epsilon \oplus \mathbb{X}^{++}_\epsilon$ we have*

$$C\cdot\|U\|_{\mathbb{L}^2(\Omega)} \leq \|U\|_{**} \leq M_{\alpha,\epsilon}\cdot\|U\|_{\mathbb{L}^2(\Omega)}.$$

Proof. The result of the local case [33, Proposition 5.4] contains the same estimates provided in this lemma. Although the norm for the mixed case is not the same as the norm used in the local case, the norms are similar by Lemma 4.5. Careful examination of the details of [33, Proposition 5.4] reveal an application to the mixed case considered here. The estimates in [33, Proposition 5.4] rely upon [33, Lemma 3.4], [33, Corollary 5.2], $\|\cdot\|_*-$norm [33, (18)], and a complete set of eigenfunctions of the linearization [33, Proposition 3.7]. Again, the $\|\cdot\|_{**}-$norm considered here is similar to the $\|\cdot\|_*$. Assumptions 4.2 and 4.3, along with asymptotic growth rate of $\nu_{k,\epsilon}$ given by (3.10) yield the analogous forms of [33, Corollary 5.2]. Furthermore, the asymptotic growth of $\nu_{k,\epsilon}$ given in (3.10) shows that the asymptotic behavior of the eigenvalues of the local case [33, Lemma 3.4] is the same as for the mixed case given by Lemma 3.3. Lemma 3.4 shows that the eigenfunctions for the mixed case are also a complete set for $\mathbb{X}$. Thus, the result holds. □

The final lemma shows that the nonlinearity of the evolution equation is differentiable in the Banach setting. Furthermore, the Lipschitz constant is polynomially bounded.

Lemma 4.7 (Properties of F). *Suppose that Assumptions 2.1 - 2.14, 4.2 and 4.3 are satisfied. Let h be defined as in (4.2). Furthermore, for arbitrary $U = (u, v) \in \mathbb{X}^\alpha$ let $F(U) = h(u, v)$. Then for every α satisfying $\dim\Omega/4 < \alpha < 1$ this defines a nonlinear mapping $F : \mathbb{X}^\alpha \to \mathbb{X}$ which is continuously Fréchet differentiable. Furthermore, there exist positive constants C and R_0 such that for any $0 < R \le R_0$ the following holds. For arbitrary $U, V \in \mathbb{X}^\alpha$ with*

$$\|U - (\bar{u}_0, \bar{v}_0)\|_{**} \le R \quad \text{and} \quad \|V - (\bar{u}_0, \bar{v}_0)\|_{**} \le R,$$

we have

$$\|F(U) - F(V)\|_{\mathbb{X}} \le C \cdot R^\chi \cdot \|U - V\|_{**}. \tag{4.12}$$

Proof. The result follows directly from [33, Lemma 5.5]. Note that χ describes the smoothness of (f, g) as given by Assumption 2.11. □

We now have everything that we need to prove the result for early pattern formation, schematically depicted in Fig. 8.

Theorem 4.8 (Early Pattern Formation). *For System (1.1), suppose that Assumptions 2.1 - 2.14, 4.2 and 4.3 are satisfied. Choose α such that $\dim\Omega/4 < \alpha < 1$ where $\mathbb{X}^\alpha = \mathbb{H}^{2\alpha}_{\text{per}}(\Omega)$. For every $0 < p \ll 1$ and $0 < d_0 \ll 1$, there exist constants ϵ_0, r_ϵ, and R_ϵ such that*

(a) *$0 < r_\epsilon < R_\epsilon$ and both constants are proportional to $\epsilon^{(2\alpha+\dim\Omega)/(2\chi)}$ as $\epsilon \to 0$.*

(b) *For all $\epsilon \le \epsilon_0$, there exists an invariant manifold $\mathcal{N}_\epsilon$ with nearly linear behavior. That is, with probability of $1 - p$ the solutions with initial conditions contained in $\mathcal{N}_\epsilon \cap B_{r_\epsilon}(\bar{u}_0, \bar{v}_0)$ leave the ball B_{R_ϵ} at a distance from $(\bar{u}_0, \bar{v}_0) + \mathbb{X}^+_\epsilon \oplus \mathbb{X}^{++}_\epsilon$ no larger than $d_0 R_\epsilon$.*

Proof of Theorem 4.8. Lemmas 4.1 - 4.7, show that hypotheses (H1)–(H3) are valid. As pointed out in Theorem [33, Theorem 5.7], pairwise orthogonality is not required to apply the theory in [26], as long as the angle between any two spaces is bounded away from 0 and π. Since Lemma 3.4 shows this to be true, we have verified everything except for the size of r_ϵ and R_ϵ.

Using [26, Remark 3.1, Lemma 3.6], as $\epsilon \to 0$, we have that $r_\epsilon/L \to C_{r_\epsilon}$ and $R_\epsilon/L \to C_{R_\epsilon}$ where L is a Lipschitz constant of the nonlinearity F. By Lemma 4.7, we have that the Lipschitz constant is given as $L = C \cdot R^\chi$, where C, R are constants. As $\epsilon \to 0$, [26, Remark 2.5] gives

$$C \cdot R^\chi \le \frac{C^{--}_\epsilon C^+_\epsilon}{2C^+_\epsilon + M_{\alpha,\epsilon} C^{--}_\epsilon}, \tag{4.13}$$

where

$$C^+_\epsilon = \frac{\min\left(b^-_\epsilon - a^-_\epsilon, b^+_\epsilon - a^+_\epsilon\right)}{6 + \chi + 1/\chi},$$

$$C^{--}_\epsilon = \frac{b^{--}_\epsilon - a^{--}_\epsilon}{2 \cdot M_{\alpha,\epsilon} + 3\sqrt{2} \cdot M^{--}_\epsilon \cdot (b^{--}_\epsilon - a^{--}_\epsilon)^\alpha}.$$

Using Lemma 4.6, we have that as $\epsilon \to 0$, $M_{\alpha,\epsilon} = C_1 \cdot \epsilon^{-\alpha}$ and $M_\epsilon^{--} \leq C_2 \cdot \epsilon^{(-\alpha-\alpha\dim\Omega/2)}$. This implies that

$$C_\epsilon^{--} \geq C_3 \cdot \epsilon^{(2\alpha+\dim\Omega)/2}, \tag{4.14}$$

$$C_\epsilon^{+} \geq d \cdot \epsilon^{(\dim\Omega/2)}. \tag{4.15}$$

Combining Estimates (4.14) and (4.15) with Estimate 4.13, we have

$$R^\chi \leq K \cdot \epsilon^{(2\alpha+\dim\Omega)/2}. \tag{4.16}$$

Since $r_\epsilon, R_\epsilon \sim R^\chi$, we get that $r_\epsilon, R_\epsilon \sim \epsilon^{(2\alpha+\dim\Omega)/(2\chi)}$. □

Theorem 4.8 shows that the addition of the nonlocal term to local diffusion produces similar early pattern results when compared to the pure local case considered in [33]. Lemma [33, Lemma 5.5] provides an initial estimate for the size of the nonlinearity F. However, this bound is improved in Proposition [33, Proposition 6.2] and we now discuss the improved estimate as it is essential for the almost linear result. Consider the regions that are given in terms of cones $(\bar{u}_0, \bar{v}_0) + \mathcal{K}_\delta$, where

$$\mathcal{K}_\delta = \{U \in \mathbb{X}^\alpha : \|U_-\|_{**} \leq \delta \|U_+\|_{**}, U = U_+ + U_- \in \mathcal{Y}_\epsilon^+ \oplus \mathcal{Y}_\epsilon^-\},$$
$$\mathcal{Y}_\epsilon^+ = \mathbb{X}_\epsilon^+ \oplus \mathbb{X}_\epsilon^{++} \subset \mathbb{X}^\alpha, \mathcal{Y}_\epsilon^- = \left(\mathbb{X}_\epsilon^{--} \cap \mathbb{X}^\alpha\right) \oplus \mathbb{X}_\epsilon^- \subset \mathbb{X}^\alpha.$$

Using these cone regions, the improved bound is given by the following lemma that follows immediately from Proposition [33, Proposition 6.2].

Lemma 4.9. *Suppose that Assumptions 2.1 - 2.14, 4.2 and 4.3 are satisfied and let F be as defined in* (4.3). *For $\dim\Omega/4 < \alpha < 1$ and $\delta_0 > 0$, denote*

$$\delta_\epsilon = \delta_0 \cdot \epsilon^{(\alpha-\dim\Omega/4)}. \tag{4.17}$$

Then there exists $\epsilon-$independent constants M_1, $M_2 > 0$ such that for every $0 < \epsilon \leq 1$ and $U \in \mathcal{K}_{\delta_\epsilon}$, with

$$\|U\|_{**} \leq M_1 \cdot \epsilon^{(-\alpha+\dim\Omega/4)}, \tag{4.18}$$

we have

$$\|F((\bar{u}_0, \bar{v}_0) + U)\|_{\mathbb{L}^2(\Omega)} \leq M_2 \epsilon^{(\alpha-\dim\Omega/4)\cdot(\chi+1)} . \|U\|_{**}^{\chi+1} \tag{4.19}$$

The order of the zero $(\bar{u}_0, \bar{v}_0)$ of F is given by χ in Assumption 2.11.

In other words, if a solution U with initial condition $U_0 \in (\bar{u}_0, \bar{v}_0) + \mathcal{K}_{\delta_\epsilon}$, with $\delta_\epsilon = \delta_0 \cdot \epsilon^{(\alpha-\dim\Omega)}$, then it is possible for the solution to remain close to $\mathbb{X}_\epsilon^+ \oplus \mathbb{X}_\epsilon^{++}$ for larger distances away from the homogeneous equilibrium compared to the early pattern results. We now state and prove our final result.

Theorem 4.10 (Later Pattern Formation)**.** *Suppose that Assumptions 2.1–2.14, 4.2 and 4.3 are satisfied and choose and fix $\delta_0 \in (0, \frac{1}{2})$ and $0 < \xi \ll 1$. Let $\epsilon \in (0, 1]$. Choose α such that $\dim\Omega/4 < \alpha < 1$ where $\mathbb{X}^\alpha = \mathbb{H}^{2\alpha}_{\text{per}}(\Omega)$. There exists a constant D and splitting of $\mathbb{X}^\alpha$ such that the following is true. If $U_0 \in (\bar{u}_0, \bar{v}_0) + \mathcal{K}_{\delta_\epsilon}$, with $\delta_\epsilon = \delta_0 \cdot \epsilon^{(\alpha-\dim\Omega)}$ whose initial condition satisfies*

$$0 < \|U_0 - (\bar{u}_0, \bar{v}_0)\|_{**} < \min(1, (D\epsilon^{-(\alpha-\dim\Omega/4)+\alpha/\chi+\xi})^{1/(1-\xi)}), \tag{4.20}$$

then for

$$\|U(t) - (\bar{u}_0, \bar{v}_0)\|_{**} \leq D\epsilon^{-(\alpha-\dim\Omega/4)+\alpha/\chi+\xi} \cdot \|U_0 - (\bar{u}_0, \bar{v}_0)\|_{**}^{\xi},$$

the relative distance of the (u, v) *and* $(u_{\text{lin}}, v_{\text{lin}})$ *is bounded by*

$$\frac{\|U(t) - (\bar{u}_0, \bar{v}_0) - U_{\text{lin}}(t)\|_{**}}{\|U_{\text{lin}}(t)\|_{**}} \leq \frac{\delta_0}{2} \cdot \epsilon^{(\alpha - \dim \Omega/4)} \tag{4.21}$$

Proof of Theorem 4.10. Fix $0 < \beta < 1$ such that Lemma 4.3 is satisfied. Lemmas 4.1 - 4.7 are used to provide the early pattern results given by Theorem 4.8 and show that for solutions that are initially close to the unstable subspace $(\bar{u}_0, \bar{v}_0) + \mathbb{X}_\epsilon^+ \oplus \mathbb{X}_\epsilon^{++}$ remain close to this space. These lemmas show that the decomposition of the phase space for the local case is also achievable for the mixed system. Furthermore, the fractional power space used for the nonlocal case is a subset of the fractional power space used in the local case. [33, Theorem 6.3] is directly applied, thus giving the result. □

Remark 4.11. By Assumption 4.3, we have that ϵ_0 must satisfy

$$\epsilon_0^{1-\theta} < \Big(\frac{s_\ell}{(1-\beta)\hat{K}_0}\Big).$$

If $\theta = 1$, then

$$1 < \Big(\frac{s_\ell}{(1-\beta)\hat{K}_0}\Big),$$

implying that our results hold around some small interval $[\beta_0, 1]$ that contains β. This is verified by our numerical results (cf. Figure 4-6). For β values outside of this interval, only the first few finite eigenfunctions corresponding to the eigenvalues of the spectrum are contained within the unstable subspaces. Although the eigenfunctions are not as dominant as the eigenfunctions associated with higher eigenmodes, the behavior of solutions cannot be explained by considering only the a small number of the most dominant eigenfunctions. Again, this is consistent with our numerical results (cf. Figures 4-6).

5. Concluding remarks

In this paper, reaction-diffusion systems with mixed nonlocal and local diffusion terms are considered where as $\epsilon \to 0$, $\epsilon^\theta J(x) \to K(x)$, where $K(x)$ is an ϵ-independent kernel. For $0 \leq \theta \leq 1$, the initial pattern selection is dominated by linear behavior. We believe our methods can be applied to other related mixed local-nonlocal models. For example, such behavior has previously been observed numerically for phase field models with local and nonlocal diffusion terms, and we expect that similar results can be obtained with only minor adjustments of the proofs presented here. For further results on the current model, we believe that it would be possible to apply the probabilistic methods found in [37, 11] to show that later stages of pattern formation are governed by linear effects. Furthermore, we conjecture that these results are attainable on certain non-rectangular domains, as long as it is possible to define the nonlocal kernel to have even symmetry. For example, it should be possible to extend these results to the disk.

Bates and Chen [4] point out that the Laplacian is considered as a first-order approximation for pure nonlocal systems for a single space dimension. See also [6, 5]. Furthermore, it is possible to approximate the nonlocal heat equation subject to Dirichlet boundary conditions [8] and the heat equation subject to Neumann boundary conditions [9] with local diffusion. In other words, solutions of the nonlocal system are close to solutions of a local system, using the same initial conditions.

Preliminary numerics suggest that the same may also be said for System (1.1). That is, by parameterizing the kernel appropriately with respect to ϵ, the nonlocal system displays almost linear behavior as $\epsilon \to 0$. Thus for carefully chosen kernels, the results developed for the mixed case would apply to the nonlocal case as well.

6. Appendix: Kernel and nonlinearities

The numerical results in this paper all use the nonlinearities given in the system of Thomas for f and g [28]. The nonlinearities are given as

$$\begin{aligned} f(u,v) &= a - u - \frac{\rho uv}{1+u+Ku^2}, \\ g(u,v) &= A(b-v) - \frac{\rho uv}{1+u+Ku^2}, \end{aligned} \tag{6.1}$$

where a, b, ρ, A, and K are positive constants that depend upon reaction kinetics. We choose $a = 150$, $b = 100$, $\rho = 13$, $A = 1.5$, and $K = .05$. These nonlinearities satisfy conditions for a Turing instability with real eigenvalues. Furthermore, with $\chi = 1$, the Thomas system satisfies Assumption 2.11.

We consider a kernel that is similar to the kernel used in [17]. Let the Gaussian kernel $\mathcal{G}$ be defined as

$$\mathcal{G}(x,y) = \exp\left(\frac{-x^2-y^2}{\sigma^2}\right) \cdot \eta(x,y), \tag{6.2}$$

where $\eta(x,y)$ is a smooth cutoff function. The function η is 1 on $B_{1/3}(0,0)$, but vanishes outside of $B_{1/2}(0,0)$. On the domain $\Omega = [0,1]^2$, the kernel G is given as

$$G(x,y) = \frac{C}{\epsilon^\theta} \cdot \left(\mathcal{G}(x,y) + \mathcal{G}(x+1,y) + \mathcal{G}(x,y+1) + \mathcal{G}(x+1,y+1)\right). \tag{6.3}$$

Outside of $\Omega = [0,1]^2$, $J(x,y)$ is given as the smooth periodic extension of $G(x,y)$, denoted as

$$J(x,y) = G_{\text{per}}(x,y). \tag{6.4}$$

Note that $\hat{J}_0 = \frac{C}{\epsilon^\theta} \cdot \hat{\mathcal{G}}_0$. We perform numerics for the cases $\theta \to 1$ and $\theta = 1$, although not all numerics are shown. For the following computation, we fix $\theta = 1$. In this case, $\epsilon\hat{J}_0$ lies just to the right of $(s_\ell, s_r) \approx (.0071, .8806)$. For this case, we choose $\frac{C}{\epsilon}$ so that the infinitely many eigenvalues of the linearized right hand side are not all positive. The condition

$$\frac{\epsilon \cdot \frac{C}{\epsilon}\hat{\mathcal{G}}_0}{s_r} > 1, \tag{6.5}$$

or equivalently

$$\frac{C\hat{\mathcal{G}}_0}{s_r} > 1 \tag{6.6}$$

permits a finite number of eigenvalues. Note that the integral of the kernel J over $[0,1]^2$ is given as the first Fourier coefficient denoted as $\hat{J}_0$. For small σ, a good approximation for this integral is the volume of G over all $\mathbb{R}^2$. To understand why, observe that most of the support for G occurs within 3σ of each corner of $[0,1]^2$ for $\sigma \ll 1$. Thus, we can compute $\hat{J}_0$ using

$$\hat{\mathcal{G}}_0 = \int_\Omega \mathcal{G}(x)dx \approx \sigma^2\pi.$$

For $\sigma \ll 1$,

$$C = \frac{2s_r}{\sigma^2\pi}. \tag{6.7}$$

Choosing $\sigma = .1$ is sufficient for our purposes. Thus from (6.7),

$$C = 200 \cdot \frac{s_r}{\pi}. \tag{6.8}$$

Note that

$$\lim_{\epsilon\to 0} \epsilon \cdot \hat{J}_0 = 2s_r > 0.$$

Acknowledgments. We want thank the anonymous referees, whose careful comments helped to significantly improve this article.

E. Sander was partially supported by NSF Grants DMS-0639300 and DMS-0907818, as well as NIH Grant R01-MH79502. R. Tatum was partially supported by the Office of Naval Research In-house Laboratory Independent Research Program.

References

[1] Y. A. Abramovich and C. D. Aliprantis. *An Invitation to Operator Theory*. American Mathematical Society, Providence RI, 2002.

[2] N. D. Alikakos, L. Bronsard, and G. Fusco. Slow motion in the gradient theory of phase transitions via energy and spectrum. *Calculus of Variations and Partial Differential Equations*, 6:39–66, 1998.

[3] W. Arendt and W. P. Schleich. *Mathematical Analysis of Evolution, Information and Complexity*. Wiley-VCH, Germany, 2009.

[4] P. Bates and F. Chen. Spectral analysis and multidimensional stability of traveling waves for nonlocal Allen-Cahn equation. *J. Math. Anal. Appl.*, 273:45–57, 2001.

[5] P. Bates, F. Chen, and J. Wang. *Global existence and uniqueness of solutions to a nonlocal phase-field system: in P.W. Bates, S.-.N Chow, K. Lu, X. Pan (Eds)*. International Press, Cambridge, MA, 1997. 14-21 pp.

[6] P. Bates, P. Fife, R. Gardner, and C. Jones. The existence of traveling wave solutions of a generalized phase-field model. *SIAM J. Math. Anal.*, 28:60–93, 1997.

[7] H. Berestycki, G. Nadin, B. Perthame, and L. Ryzhik. The nonlocal Fisher-KPP equation: traveling waves and steady states. *Nonlinearity*, 22:2813–2844, 2009.

[8] C. Cortazar, M. Elgueta, and J. Rossi. Nonlocal diffusion problems that approximate the heat equation with Dirichlet boundary conditions. *Israel Journal of Mathematics*, 170(1): 53–60, 2009.

[9] C. Cortazar, M. Elgueta, J. Rossi, and N. Wolanski. How to approximate the heat equation with Neumann boundary conditions by nonlocal diffusion problems. *Archive for Rational Mechanics and Analysis*, 187(1):137–156, 2008.

[10] R. Courant and D. Hilbert. *Methods of Mathematical Physics*. Interscience Publishers, Inc., New York, 1989.

[11] J. P. Desi, E. Sander, and T. Wanner. Complex transient patterns on the disk. *Discrete and Continuous Dynamical Systems*, 15(4):1049–1078, 2006.

[12] K. Engel and R. Nagel. *One-Parameter Semigroups for Linear Evolution Equations*. Springer-Verlag, New York, 2000.

[13] R. J. Field and R. M. Noyes. Oscillations in chemical systems. IV. Limit cycle behaviour in a model of a real chemical reaction. *J. Chem. Phys.*, 60:1877–1884, 1974.

[14] P. Fife. Some nonclassical trends in parabolic and parabolic-like evolutions. In *Trends in nonlinear analysis*, pages 153–191. Springer, Berlin, 2003.

[15] C. P. Grant. Spinodal decomposition for the Cahn-Hilliard equation. *Communications in Partial Differential Equations*, 18:453–490, 1993.

[16] T. Hartley. An analysis of phase separation processes for stochastic and nonlocal extensions of the classical phase field model. GMU, 2008.

[17] T. Hartley and T. Wanner. A semi-implicit spectral method for stochastic nonlocal phase-field models. *Discrete and Continuous Dynamical Systems, A*, 25:399–429, 2009.

[18] D. Henry. *Geometric Theory of Semilinear Parabolic Equations*. Springer–Verlag, New York, 1981.
[19] M. Hildebrand, H. Skødt, and K. Showalter. Spatial symmetry breaking in the Belousov-Zhabotinksy reaction with light-induced remote communication. *Phys. Rev. Lett.*, 87(8):1–4, 2001.
[20] E. K. Infantis and P. N. Panagopoulos. Limit points of eigenvalues of truncated tridiagonal operators. *J. Comp. and Appl. Math.*, 133:413–422, 2001.
[21] T. Kato. *Perturbation Theory for Linear Operators*. Springer-Verlag, Heidelberg, 1976.
[22] Y. Katznelson. *Introduction to Harmonic Analysis*. Cambridge University Press, United Kingdom, 2004.
[23] C. Lederman and N. Wolanski. Singular perturbation in a nonlocal diffusion problem. *Communications in Partial Differential Equations*, 31(1-3):195–241, 2006.
[24] I. Lengyel and I. R. Epstein. A chemical approach to designing Turing patterns in reaction-diffusion systems. *Proc. Natl. Acad. Sci., USA*, 89:3977–3979, 1992.
[25] S. Maier-Paape and T. Wanner. Spinodal decomposition of the Cahn-Hilliard equation in higher dimensions. part I: probability and wavelength estimate. *Comm. Math. Phys.*, 195(2): 435–464, 1998.
[26] S. Maier-Paape and T. Wanner. Spinodal decomposition for the Cahn-Hilliard equations in higher dimensions: nonlinear dynamics. *Arch. Rational Mech. Anal.*, 151(3):187–219, 2000.
[27] J. Murray. A prepattern formation mechanism for animal coat markings. *Journal of Theoretical Biology*, 88:161–199, 1981.
[28] J. D. Murray. *Mathematical Biology, Vol. I, An Introduction*. Springer–Verlag, New York, third edition, 1993.
[29] J. D. Murray. *Mathematical Biology, Vol. II, Spatial Models and Biomedical Applications*. Springer–Verlag, New York, third edition, 1993.
[30] M. G. Neubert, H. Caswell, and J. D. Murray. Transient dynamics and pattern formation: reactivity is necessary for Turing instabilities. *Math. Biosci.*, 175(1):1–11, 2002.
[31] A. Pazy. *Semigroups of Linear Operators and Applications to Partial Differential Equations. Applied Mathematical Sciences*, volume 44. Springer–Verlag, New York, 1983.
[32] M. Renardy and R. C. Rogers. *An Introduction to Partial Differential Equations*. Springer–Verlag, New York, second edition, 2004.
[33] E. Sander and T. Wanner. Pattern formation in a nonlinear model for animal coats. *Journal of Differential Equations*, 191:143–174, 2003.
[34] E. S. Suhubi. *Functional Analysis*. Kluwer Academic Publishers, Norwell, Massachusettes, first edition, 2003.
[35] A. Turing. The chemical basis of morphogenesis. *Philosophical Transactions of the Royal Society of London. Series B, Biological Sciences*, 237:37–72, 1952.
[36] V. K. Vanag and I. R. Epstein. Pattern formation in a tunable reaction-diffusion medium: the BZ reaction in an aerosol OT microemulsion. *Phys. Rev. Lett.*, 87:1–4, 2001.
[37] T. Wanner. Maximum norms of random sums and transient pattern formation. *Transactions of the American Mathematical Society*, 356(6):2251–2279, 2004.

Evelyn Sander
Department of Mathematical Sciences, George Mason University, 4400 University Dr., Fairfax, VA, 22030, USA
E-mail address: esander@gmu.edu

Richard Tatum
Naval Surface Warfare Center Dahlgren Division, 18444 Frontage Road Suite 327, Dahlgren, VA 22448-5161, USA
E-mail address: rchrd.ttm@gmail.com